



NAVAL POSTGRADUATE SCHOOL

MONTEREY, CALIFORNIA

THESIS

**EXPERIMENTAL INVESTIGATION OF HIGH-PRESSURE
STEAM-INDUCED SURGE IN A TRANSONIC
COMPRESSOR STAGE**

by

Andrew M. Hurley

June 2008

Thesis Advisor:
Second Reader:

Anthony Gannon
Garth Hobson

Approved for public release; distribution is unlimited

THIS PAGE INTENTIONALLY LEFT BLANK

REPORT DOCUMENTATION PAGE			<i>Form Approved OMB No. 0704-0188</i>	
Public reporting burden for this collection of information is estimated to average 1 hour per response, including the time for reviewing instruction, searching existing data sources, gathering and maintaining the data needed, and completing and reviewing the collection of information. Send comments regarding this burden estimate or any other aspect of this collection of information, including suggestions for reducing this burden, to Washington headquarters Services, Directorate for Information Operations and Reports, 1215 Jefferson Davis Highway, Suite 1204, Arlington, VA 22202-4302, and to the Office of Management and Budget, Paperwork Reduction Project (0704-0188) Washington DC 20503.				
1. AGENCY USE ONLY (Leave blank)		2. REPORT DATE June 2008	3. REPORT TYPE AND DATES COVERED Master's Thesis	
4. TITLE AND SUBTITLE Experimental Investigation of High-Pressure Steam-Induced Surge in a Transonic Compressor Stage			5. FUNDING NUMBERS	
6. AUTHOR(S) Andrew M. Hurley				
7. PERFORMING ORGANIZATION NAME(S) AND ADDRESS(ES) Naval Postgraduate School Monterey, CA 93943-5000			8. PERFORMING ORGANIZATION REPORT NUMBER	
9. SPONSORING /MONITORING AGENCY NAME(S) AND ADDRESS(ES) N/A			10. SPONSORING/MONITORING AGENCY REPORT NUMBER	
11. SUPPLEMENTARY NOTES The views expressed in this thesis are those of the author and do not reflect the official policy or position of the Department of Defense or the U.S. Government.				
12a. DISTRIBUTION / AVAILABILITY STATEMENT Approved for public release; distribution is unlimited			12b. DISTRIBUTION CODE	
13. ABSTRACT (maximum 200 words) <p>Operational experience indicates that steam escaping from carrier catapults has the potential to induce stall or surge in the compressors of jet aircraft during takeoff. As the carrier fleet ages and the Navy transitions to the single engine F-35C variant of the Joint Strike Fighter, further investigation of steam-induced surge phenomena is necessary to avert undue risks to pilots and to obviate stall related damage to Navy aircraft. This study investigated the effects of both throttle-induced surge and steam-induced surge in a transonic compressor stage at 70%, 80%, 90%, 95%, and 100% of the compressor design speed. The primary goals of this research were to quantify changes in the compressor stall margin as a result of steam ingestion and to develop pressure contour maps to analyze the transformation of shock structures in the blade passages as they relate to inlet throttle settings. The results of this experiment confirmed that the introduction of high-pressure steam consistently reduced the observed compressor stall margin over the entire operating range of the transonic stage and produced reliable representations of the shock structure present along the compressor casing.</p>				
14. SUBJECT TERMS Compressor, Transonic, Steam Ingestion, Stall, Surge			15. NUMBER OF PAGES 65	
			16. PRICE CODE	
17. SECURITY CLASSIFICATION OF REPORT Unclassified	18. SECURITY CLASSIFICATION OF THIS PAGE Unclassified	19. SECURITY CLASSIFICATION OF ABSTRACT Unclassified	20. LIMITATION OF ABSTRACT UU	

THIS PAGE INTENTIONALLY LEFT BLANK

Approved for public release; distribution is unlimited

**EXPERIMENTAL INVESTIGATION OF HIGH-PRESSURE STEAM-INDUCED
SURGE IN A TRANSONIC COMPRESSOR STAGE**

Andrew M. Hurley
Ensign, United States Navy
B.S., United States Naval Academy, 2007

Submitted in partial fulfillment of the
requirements for the degree of

MASTER OF SCIENCE IN MECHANICAL ENGINEERING

from the

**NAVAL POSTGRADUATE SCHOOL
June 2008**

Author: Andrew M. Hurley

Approved by: Prof. Anthony J. Gannon
Thesis Advisor

Prof. Garth V. Hobson
Second Reader

Dr. Anthony Healey
Chairman
Department of Mechanical and Aeronautical Engineering

THIS PAGE INTENTIONALLY LEFT BLANK

ABSTRACT

Operational experience indicates that steam escaping from carrier catapults has the potential to induce stall or surge in the compressors of jet aircraft during takeoff. As the carrier fleet ages and the Navy transitions to the single engine F-35C variant of the Joint Strike Fighter, further investigation of steam-induced surge phenomena is necessary to avert undue risks to pilots and to obviate stall related damage to Navy aircraft. This study investigated the effects of both throttle-induced surge and steam-induced surge in a transonic compressor stage at 70%, 80%, 90%, 95%, and 100% of the compressor design speed. The primary goals of this research were to quantify changes in the compressor stall margin as a result of steam ingestion and to develop pressure contour maps to analyze the transformation of shock structures in the blade passages as they relate to inlet throttle settings. The results of this experiment confirmed that the introduction of high-pressure steam consistently reduced the observed compressor stall margin over the entire operating range of the transonic stage and produced reliable representations of the shock structure present along the compressor casing.

THIS PAGE INTENTIONALLY LEFT BLANK

TABLE OF CONTENTS

I.	INTRODUCTION.....	1
II.	STALL THEORY	3
	A. ROTATING STALL.....	3
	B. SURGE.....	4
	C. HYSTERESIS	4
III.	EXPERIMENTAL APPARATUS.....	7
	A. TRANSONIC COMPRESSOR RIG.....	7
	B. STEAM INGESTION SYSTEM	9
	C. DATA ACQUISITION SYSTEM	10
	1. Low-Speed Data Acquisition Instrumentation.....	10
	2. High-Speed Data Acquisition Instrumentation.....	11
IV.	EXPERIMENTAL PROCEDURE.....	13
	A. COMPRESSOR MAP	13
	B. STEAM INGESTION OPERATION	14
V.	RESULTS	15
	A. COMPRESSOR MAP	15
	B. STEAM INGESTION PLOTS.....	17
	C. HIGH-SPEED INSTRUMENTATION RESULTS	18
	1. Steady State Contour Plots	18
	2. Kulite Transient Data	22
VI.	CONCLUSIONS	25
VII.	RECOMMENDATIONS.....	27
	LIST OF REFERENCES.....	29
	APPENDIX A: STEAM INGESTION TIME TRACES.....	31
	APPENDIX B: MATLAB CODES USED TO PROCESS KULITE DATA	33
	APPENDIX C: PRESSURE CONTOUR PLOTS	35
	APPENDIX D: KULITE SIGNAL VOLTAGE AND ROTOR OVERSPEED DURING SURGE.....	39
	INITIAL DISTRIBUTION LIST	49

THIS PAGE INTENTIONALLY LEFT BLANK

LIST OF FIGURES

Figure 1.	Steam-Induced Stall During F-18D Takeoff at Lakehurst.....	2
Figure 2.	TPL Transonic Stage Configuration	7
Figure 3.	TPL Transonic Compressor Rig Schematic.....	9
Figure 4.	Steam Ingestion System.....	10
Figure 5.	Data Acquisition System Schematic.....	11
Figure 6.	Kulite Probes Mounted Around Compressor Annulus	12
Figure 7.	Kulite Probe Locations Relative To The Rotor Cross Section	12
Figure 8.	Pressure Ratio Map Showing Stage Surge Characteristics with Steam Ingestion.....	15
Figure 9.	Efficiency Map Showing Stage Surge Characteristics with Steam Ingestion.....	16
Figure 10.	Comparison of Rotor-Only and Stage Stall Characteristics	17
Figure 11.	Steam Ingestion Time Trace	18
Figure 12.	Interpolated Pressure Contour Maps Near Throttle-Induced Surge	19
Figure 13.	Pressure Contour Plot Progression for 70% Compressor Speed	20
Figure 14.	Pressure Contour Plot Progression for 95% Compressor Speed	21
Figure 15.	Example Plot of Raw Kulite Voltage During Steam Surge.....	22
Figure 16.	Example Plot of Rotor Speed During Steam Surge	23
Figure 17.	70% Steam Induced Surge	31
Figure 18.	80% Steam Induced Surge.....	31
Figure 19.	90% Steam Induced Surge.....	32
Figure 20.	95% Steam Induced Surge	32
Figure 21.	Pressure Contour Plot Progression for 80% Compressor Speed	35
Figure 22.	Pressure Contour Plot Progression for 90% Compressor Speed	36
Figure 23.	Pressure Contour Plot Progression for 100% Compressor Speed	37
Figure 24.	70% Throttle-Induced Surge.....	41
Figure 25.	70% Steam-Induced Surge.....	42
Figure 26.	80% Throttle-Induced Surge.....	43
Figure 27.	80% Steam-Induced Surge.....	44
Figure 28.	90% Throttle-Induced Surge.....	45
Figure 29.	90% Steam-Induced Surge.....	46
Figure 30.	95% Throttle-Induced Surge.....	47
Figure 31.	95% Steam-Induced Surge.....	48

THIS PAGE INTENTIONALLY LEFT BLANK

LIST OF TABLES

Table 1.	Sanger Stage Design Parameters	8
Table 2.	Steady State Transonic Compressor Speeds	13
Table 3.	Stall/Surge Margin Reduction Resulting from Steam Ingestion.....	16
Table 4.	Rotor Overspeed Comparison.....	23

THIS PAGE INTENTIONALLY LEFT BLANK

ACKNOWLEDGMENTS

The completion of this work would not have been possible without the commitment and expertise of the teachers and staff at the NPS Turbopropulsion Lab. The dedication and enthusiasm of my primary advisor, Prof. Anthony Gannon, created a pleasant working environment and served as a constant source of motivation. The experience of Prof. Garth Hobson was also a great blessing as his guidance contributed greatly to the quality of the work. Additionally, John Gibson and Doug Seivwright deserve a special thanks for all the time and effort invested in the data collection and maintenance of the compressor rig. Most of all, I would like to thank my family for their steadfast support in every endeavor I undertake.

THIS PAGE INTENTIONALLY LEFT BLANK

I. INTRODUCTION

Both stall and surge are well documented phenomena that reduce the operational effectiveness of compressors and pose a considerable threat of damage to essential turbomachine components. In recent years, the issue of stall precipitated by steam ingestion has garnered significant interest from the U.S. Navy. The carrier fleet continues to rely on steam catapults to facilitate aircraft launches, but the age of such systems has become evident as pressurized steam manages to vent onto the flight deck through worn steam seals. Operational experience indicates that the ingestion of high-pressure steam is capable of inducing a stall event in legacy jet engine powered aircraft, an effect that has become known as “pop-stall” as demonstrated in the F-18D takeoff featured in Figure 1. In recent years, the transition to the F35C Joint Strike Fighter (JSF) has increased the Navy’s interest in steam-induced stall phenomena due to concerns of increased vulnerability to stall in single engine platforms. In addition to a highly loaded compressor, the F35C also features serpentine inlet passages ahead of the engine which further distort the flow entering the compressor and may potentially contribute to an increase in stall susceptibility when coupled with steam present during carrier launches.

Current research in the Turbopropulsion Laboratory (TPL) at the Naval Postgraduate School (NPS) has focused upon the effect of steam-induced surge on a transonic compressor stage. This study is a continuation of the experimental results achieved by Payne, Zarro, and Koessler all of which investigated steam-induced stall phenomena in the rotor-only configuration [8, 10, 13]. The stage components implemented in this study were designed specifically for use in the TPL transonic compressor rig by Sanger at the NASA Glenn Research Center [11]. An updated compressor map was developed to document the performance of the compressor stage between 70% and 100% of the compressor design speed. Using the established compressor map as a baseline performance characteristic, the effect of high-pressure steam ingestion on the compressor stall margin was then investigated at 70%, 80%, 90%, and 95% of the design speed. The transient effects observed during surge were also analyzed using measurements from Kulite pressure transducers to provide high-speed

data capabilities. The results of the experiment showed a consistent reduction in the stall margin across the entire range of operating speeds as a result of steam-ingestion, and the rotor over speed occurring as a consequence of stalled operating conditions was quantified for steam-induced surge and throttle-induced surge.



Figure 1. Steam-Induced Stall During F-18D Takeoff at Lakehurst

II. STALL THEORY

Stall is an event that occurs in compressors when the angle of incidence on a blade reaches a critical point where the adverse pressure gradient on the suction surface precipitates flow separation. The separated flow typically results in the deterioration of compressor performance and lower pressure ratios due to decreased mass flow. In addition to the associated performance reductions, stall is an inherently violent event that can cause catastrophic failure in turbomachinery as a result of fatigue failure. Stall can be divided into two main categories which include rotating stall and surge.

A. ROTATING STALL

Rotating stall occurs when the flow separation in the compressor allows the formation of one or more localized regions of stalled flow that rotate about the compressor annulus. The perceived rotation occurs due to the fact that the localized stall cell creates a flow disturbance that overloads one of the adjacent blades while simultaneously unloading the other neighboring blade. The altered angle of incidence causes the overloaded blade to stall while the previously stalled blade is allowed to recover [7]. Although the average mass flow over the compressor cross section remains stable with respect to time, the local mass flow changes as the stall cells rotate about the cross section [1]. Rotating stall can be separated into two distinct classifications: progressive stall and abrupt stall.

Progressive stall occurs as separation in the tip region of the rotor or stator blades causes the formation of one or more part span stall cells. It is often difficult to detect progressive stall as the resulting degradation in performance is usually very small, but changes in noise during operation serves as the primary indicator in the absence of high-frequency instrumentation inside the machine [1]. The perceived rotation of part span stall cells is generally 50 to 70% of the blade speed, and the cells are usually limited to localized regions due to the ample opportunity for the circumferential redistribution of flow between stalled and unstalled regions [9].

The formation of a full span rotating stall cell is indicative of abrupt stall which results in an appreciable reduction in the compressor pressure rise and mass flow rate. Unlike progressive stall, full span stall cells may cover multiple blades over the entire length of the compressor while rotating at 40% to 80% of the rotor speed [4]. The effect of abrupt stall is also much more damaging than its counterpart as significant vibratory stresses can develop, particularly if the frequencies present correspond with the resonant frequencies of the blades [9].

B. SURGE

Surge is a phenomenon that occurs when boundary layer separation interrupts the compressor flow field in a manner that leads to violent, periodically steady pressure oscillations in a turbomachine stage [7]. Flow distortions resulting from a stalled rotor or stator precipitate conditions that force the adjacent stage component into stall. Upon stalling accompanying component, the previously stalled stage element is allowed to recover from stall; however, the ensuing flow distortions that accompany the newly stalled element perpetuate the alternating stall cycle within the stage. Although some cases of surge may only generate mild dynamic instabilities, the cyclic nature of surge has the potential to engender intense periodic pressure oscillations, excessive transverse loads on the rotor and casing, and a pronounced decline in compressor performance [7]. In the most severe occurrences, known as “deep surge”, it is even possible that a complete reversal in the mass flow forces previously compressed gas through the compressor inlet [1]. The pressure oscillations that occur during surge pose a significant threat to compressor blades due to their susceptibility to fatigue failure and engine components incapable of accommodating unsteady thrust loads.

C. HYSTERESIS

Hysteresis is an effect that manifests itself in the recovery from a compressor stall. Due to hysteresis, compressors often require a much larger throttle opening to recover from stalled operation than the throttle setting employed at the inception of a stall event [1]. For some compressor designs, the effect of hysteresis is so pronounced that it becomes necessary to perform a complete shut down and restart on the engine to resume

standard operation. Because hysteresis is primarily a function of the compressor flow coefficient, the severity of its effect is inextricably linked to the overall design of the compressor. In physical terms, the value of the compressor flow coefficient is related to the blade stagger [1]. Engineers designing compressors are faced with a difficult tradeoff as increasing the flow coefficient results in increased stage pressure ratios along with a more pronounced hysteresis effect.

THIS PAGE INTENTIONALLY LEFT BLANK

III. EXPERIMENTAL APPARATUS

A. TRANSONIC COMPRESSOR RIG

Unlike recent studies performed by Payne, Zarro, and Koessler, the transonic compressor configuration employed during this study utilized a complete stage consisting of the rotor and stator designed by NASA [8, 10, 11, 12, 13]. The experimental stage configuration is shown in Figure 2 below.

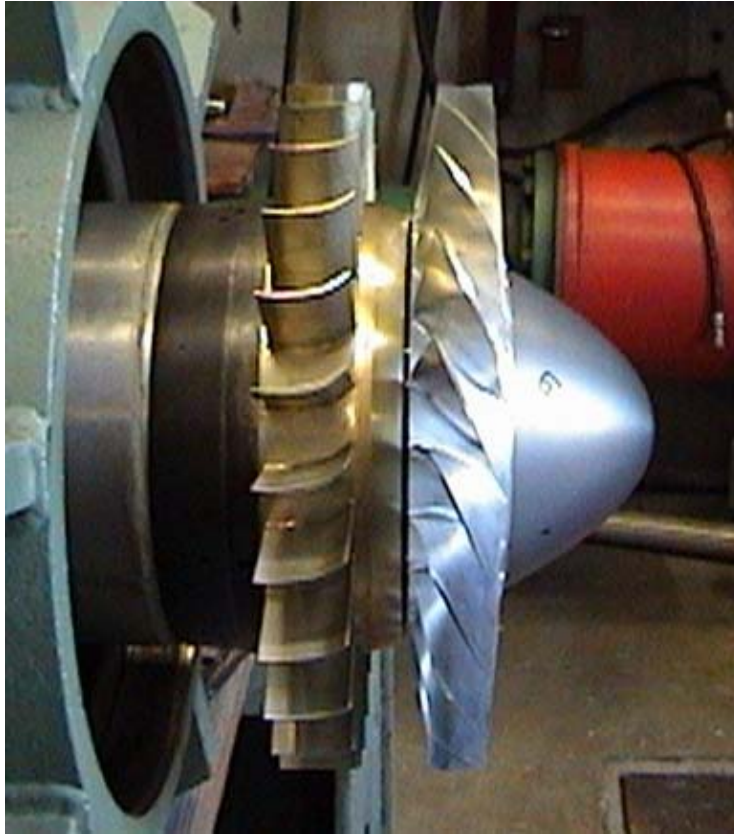


Figure 2. TPL Transonic Stage Configuration

The transonic compressor stage at NPS employed a 22 blade rotor and a 27 blade stator featuring controlled diffusion profiles. Both stage components were fabricated using a 7075-T6 aluminum alloy based on its desirable combination of strength and light weight. While a more detailed explanation of the stage design process was previously presented by Sanger, relevant stage design parameters were included in Table 1 [11, 12].

Table 1. Sanger Stage Design Parameters

Rotor Pressure Ratio	1.61
Stage Pressure Ratio	1.56
Tip Speed	396.2 m/sec
Design Speed	27,085 rpm
Design Mass Flow	7.75 kg/sec
Specific Mass Flow	170.9 kg/sec-m ²
Specific Head Rise	0.246
Tip Inlet Relative Mach Number	1.28
Aspect Ratio	1.2
Hub/Tip Radius Ratio	0.51
Number of Rotor Blades	22
Number of Stator Blades	27
Tip Solidity (Rotor)	1.3
Tip Solidity (Stator)	1.0
Outside Diameter	0.2794 m
Rotor Diffusion Factor (Tip)	0.40
Rotor Diffusion Factor (Hub)	0.47
Stator Diffusion Factor (Tip)	0.52
Stator Diffusion Factor (Hub)	0.58

A schematic illustrating the arrangement of the experimental apparatus is featured in Figure 3. The compressor rotor was driven by single-stage, opposed-rotor power turbines while the pressure ratio was controlled by an electronically actuated upstream throttle. The compressed air necessary to operate the turbine was provided via a 12-stage Allis-Chalmers axial compressor. Air from the atmosphere entered through screens in an external housing before passing through the upstream throttle valve and settling chamber. Upon exiting the settling chamber, the flow was routed through a 46 cm diameter pipe before being delivered to the test compressor stage. After exiting the compressor stage, the air was exhausted radially from the rig. More comprehensive discussions outlining the transonic compressor rig operation have been provided previously in the work of Payne and Zarro [10, 13].

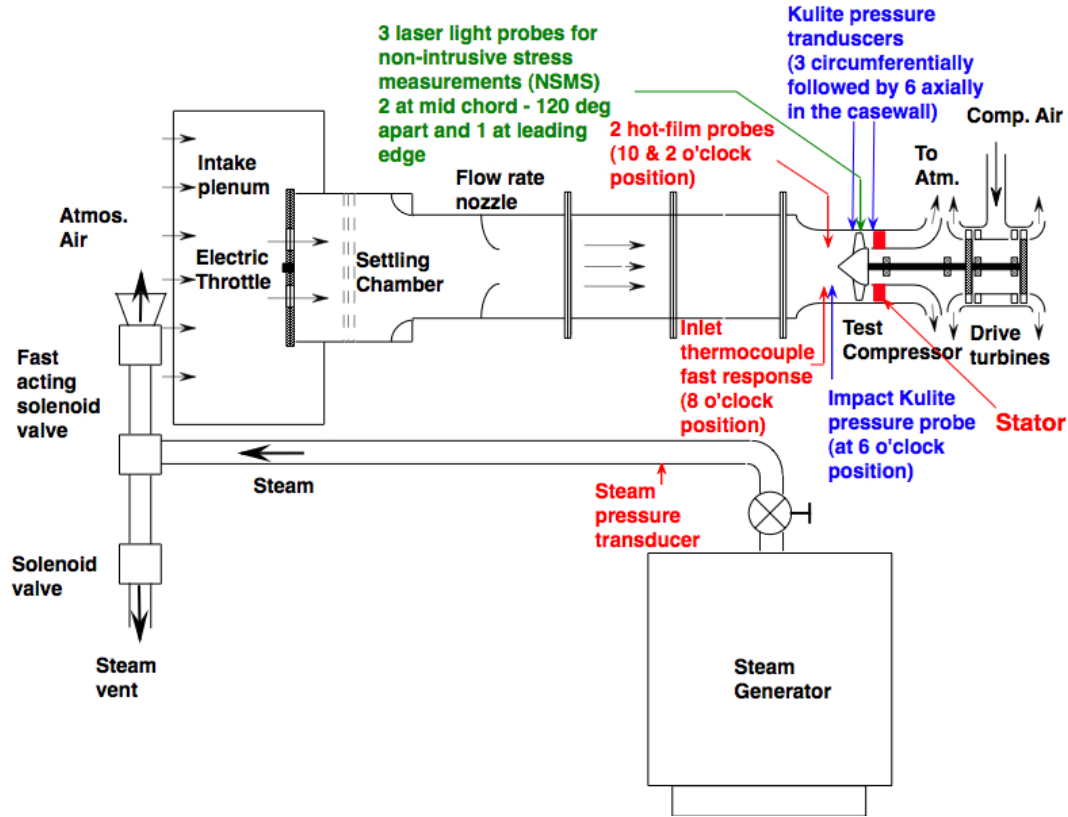


Figure 3. TPL Transonic Compressor Rig Schematic

Notable improvements to the experimental apparatus during the most recent testing included the implementation of ceramic ball bearings capable of high temperature operation and the removal of the honeycomb flow straightener previously located behind the fan [2].

B. STEAM INGESTION SYSTEM

To model the effect of steam ingestion during a carrier catapult launch, a Sussman SVS600 steam boiler was used to produce saturated steam at a pressure of 9 atm. While the steam pressure in actual catapult launches is significantly higher, general trends regarding changes in the stall margin can still be observed [3]. Figure 3 illustrates the relationship between the steam ingestion system and the compressor test apparatus, and a view of the inlet plenum and steam ingestion pipe as they appear during operation is provided in Figure 4.



Figure 4. Steam Ingestion System

During steam ingestion testing, the steam line was charged prior to each throttle adjustment. Pressure transducers in the steam line were used to ensure that the steam pressure conditions remained repeatable in subsequent trials. Once the pressure transducers verified the desired steam pressure had been achieved, activation of a solenoid valve released the steam into the inlet plenum of the compressor rig. Although the current steam pressure has been increased, the thesis work conducted by Payne and Zarro provides the technical specifications for the steam ingestion system [10, 13].

C. DATA ACQUISITION SYSTEM

The data acquisition system utilized in this experiment was comprised of both high-speed and low-speed sensors providing real-time tracking of experimental data.

1. Low-Speed Data Acquisition Instrumentation

Steady state pressure readings were captured using two upstream and 20 downstream Kiel stagnation pressure probes, while the readings from two upstream and nine downstream stagnation temperature probes were used to measure the stage isentropic efficiency. These readings were also used to calculate the mass averaged

temperature and pressure ratios of the compressor stage. The mass flow rate through the compressor was calculated from the pressure difference across the flow rate nozzle shown upstream of the compressor in Figure 3.

2. High-Speed Data Acquisition Instrumentation

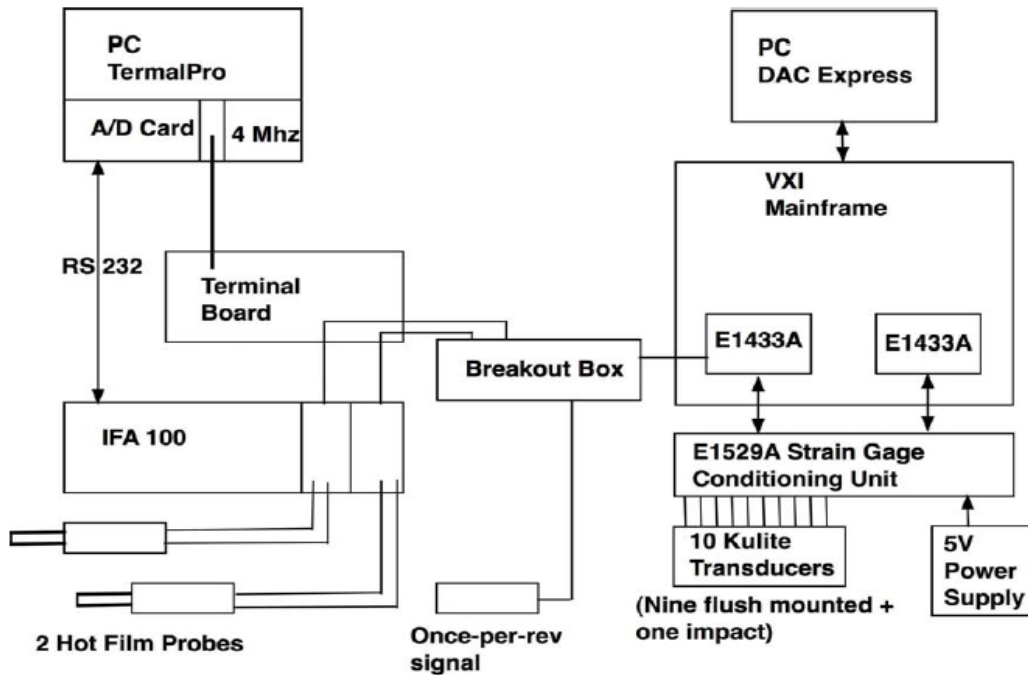


Figure 5. Data Acquisition System Schematic

The high-speed instrumentation utilized in the transonic compressor rig included one upstream impact and nine static Kulite pressure probes along with two TSI hot-film probes. These devices were integrated into the high-speed data acquisition system as illustrated in the system schematic featured in Figure 5. The nine Kulite probes, located as shown in Figures 6 and 7, were implemented to record the static pressure along the casing before and during stall events while the TSI hot-film probes were employed to measure the instantaneous velocity of the flow upstream of the stage. Both sets of probes were sampled at 196.6 kHz to thwart the aliasing of high frequencies [5]. Detailed

information regarding the technical specifications of the high speed instrumentation and their corresponding implementation methodologies has been comprehensively addressed in the work of Zarro [13].



Figure 6. Kulite Probes Mounted Around Compressor Annulus

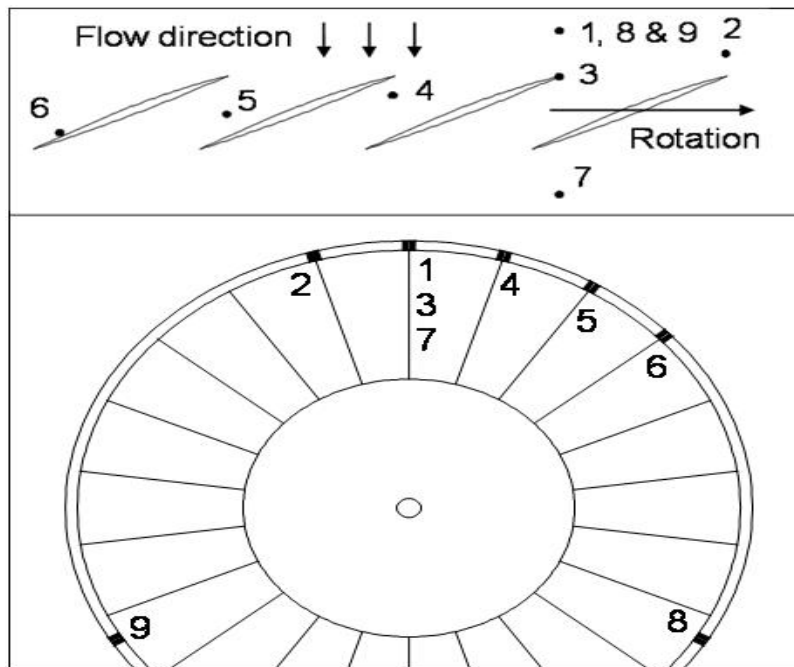


Figure 7. Kulite Probe Locations Relative To The Rotor Cross Section

IV. EXPERIMENTAL PROCEDURE

A. COMPRESSOR MAP

To establish the standard performance characteristics of the stage, it was necessary to generate a compressor map documenting the mass flow rates, pressure ratios, and isentropic efficiencies encountered between open throttle and stall over a range of operating speeds. Compressor maps documenting the performance of the rotor-only configuration were established previously in the works of Payne and Zarro [10, 13]. The speeds chosen for this research included 70%, 80%, 90%, 95%, and 100% of the compressor's operational capacity as indicated in Table 2. While maintaining a constant rotor speed, the compressor mass flow rate was controlled by incremental adjustments of the upstream throttle. At each operating point, the low-speed data acquisition system continuously updated information including the compressor speed, pressure, temperature, and the inlet mass flow at that particular throttle setting. Beyond the peak efficiency point for each speed curve, the elements of the high-speed data acquisition system were prepared and the subsequent throttle changes were reduced in anticipation of a surge event. When the surge point for a given speed was reached, a 30 second recording of the transient data was stored in a spreadsheet format and exported from the VXI mainframe. Due to the possibility of damaging the compressor as a result of overspeed during surge, only throttle-induced surge was recorded at 100% design speed.

Table 2. Steady State Transonic Compressor Speeds

Percent Speed	RPM
100%	27,085
95%	25,730
90%	24,375
80%	21,670
70%	18,960

B. STEAM INGESTION OPERATION

Upon completing the compressor map for the stage configuration, the compressor performance and surge characteristics were then evaluated based on the introduction of pressurized steam. Using the surge line developed in the compressor map as a reference, the throttle was closed to create near surge conditions, and steam from the boiler was directed into the steam piping. Once the pressure transducers in the steam pipe indicated that the desired pressure of 9 atm had been achieved, the boiler isolation valve was closed. Prior to releasing the pressurized steam into the inlet plenum of the compressor, the high-speed data acquisition system was set to begin recording data. The solenoid valve was then released allowing the pressurized steam to enter the compressor inlet, and data collection continued for a period of 30 seconds. If the pressurized steam failed to induce a surge event, the upstream throttle setting was closed and the procedure was repeated until surge was achieved.

V. RESULTS

A. COMPRESSOR MAP

A compressor map was generated to document the steady state performance of the transonic compressor stage and to locate the onset of surge as a consequence of throttle adjustment and steam ingestion. Figure 8 represents the relationship between the pressure ratio across the stage and the mass flow while Figure 9 demonstrates the relationship between the stage efficiency and the mass flow.

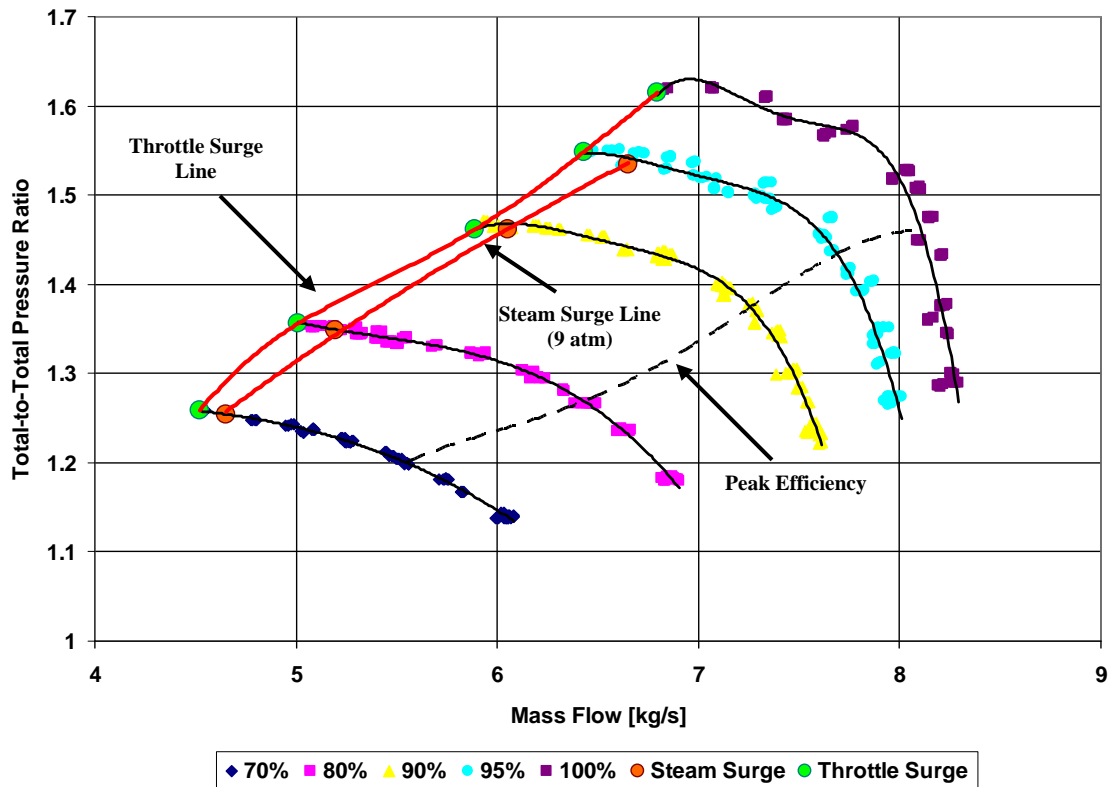


Figure 8. Pressure Ratio Map Showing Stage Surge Characteristics with Steam Ingestion

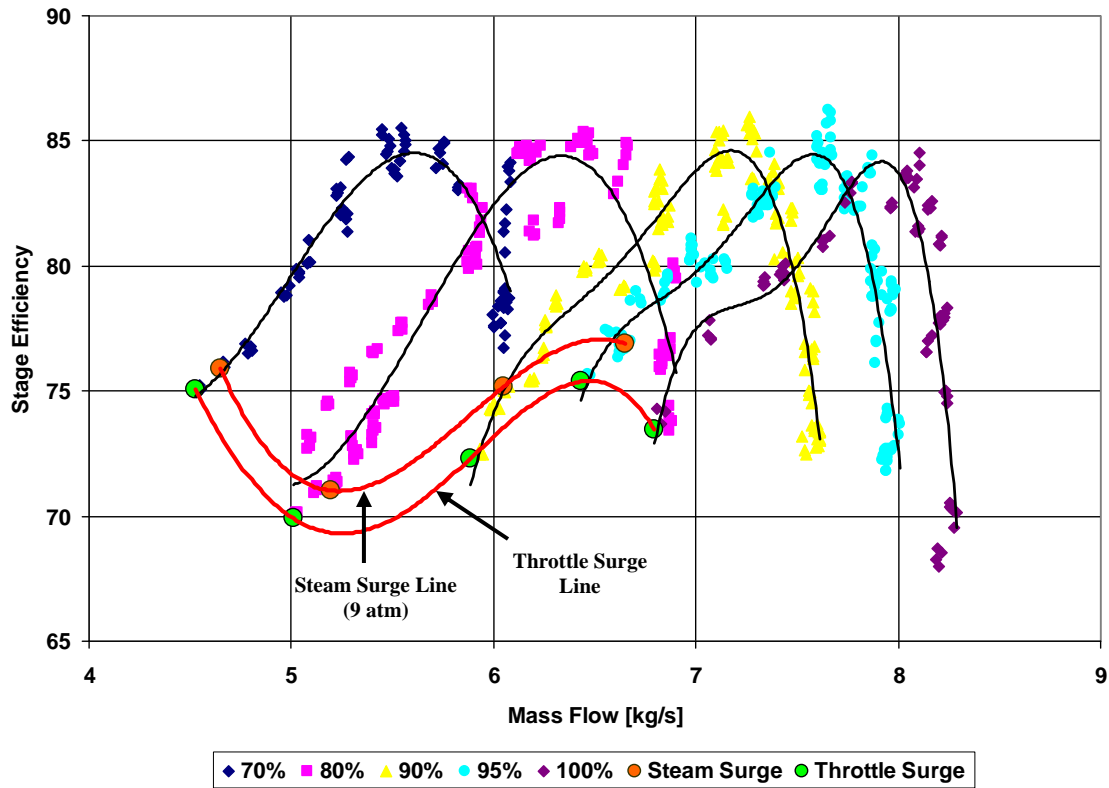


Figure 9. Efficiency Map Showing Stage Surge Characteristics with Steam Ingestion

Table 3. Stall/Surge Margin Reduction Resulting from Steam Ingestion

Rotor Speed	Stall Margin	Steam Ingestion Surge Margin	SM Reduction
70%	18.5%	16.4%	11.3%
80%	21.6%	18.6%	13.9%
90%	19.3%	17.0%	11.9%
95%	15.5%	14.0%	9.7%

Stall margins and surge margins were computed from the preceding figures by comparing the difference in the mass flow between peak efficiency and the onset of stalled operation to the total mass flow rate at peak efficiency. As shown in Table 3, the surge margin in the transonic stage was reduced by an average of 11.7% due to the introduction of pressurized steam at the compressor inlet. The relative consistency

observed in the surge margin reduction across the entire operating range of the stage was markedly different from the results obtained by Koessler in a study of the rotor-only configuration [8]. As demonstrated in Figure 10, the effect of steam ingestion on the stall margin in the rotor-only configuration diminished with increasing compressor speeds.

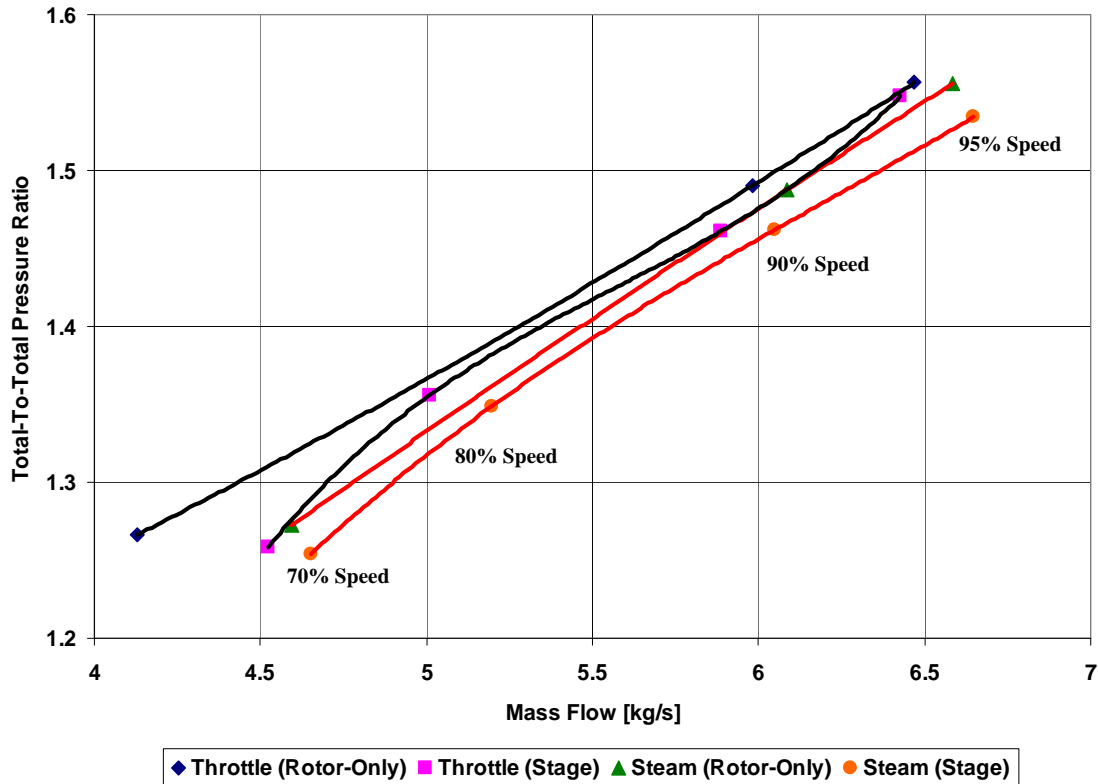


Figure 10. Comparison of Rotor-Only and Stage Stall Characteristics

B. STEAM INGESTION PLOTS

During compressor tests incorporating steam ingestion, the low-speed instrumentation recorded the rotor speed and the inlet temperature while a transducer in the steam pipe monitored changes in the steam pressure. Figure 11 features an example of the plots used to monitor the short term effects of steam ingestion on the compressor operation. This plot demonstrates the momentary spike in the compressor inlet temperature and the increase in rotor speed resulting from the injection of pressurized steam. The complete collection of steam plots is included in Appendix A.

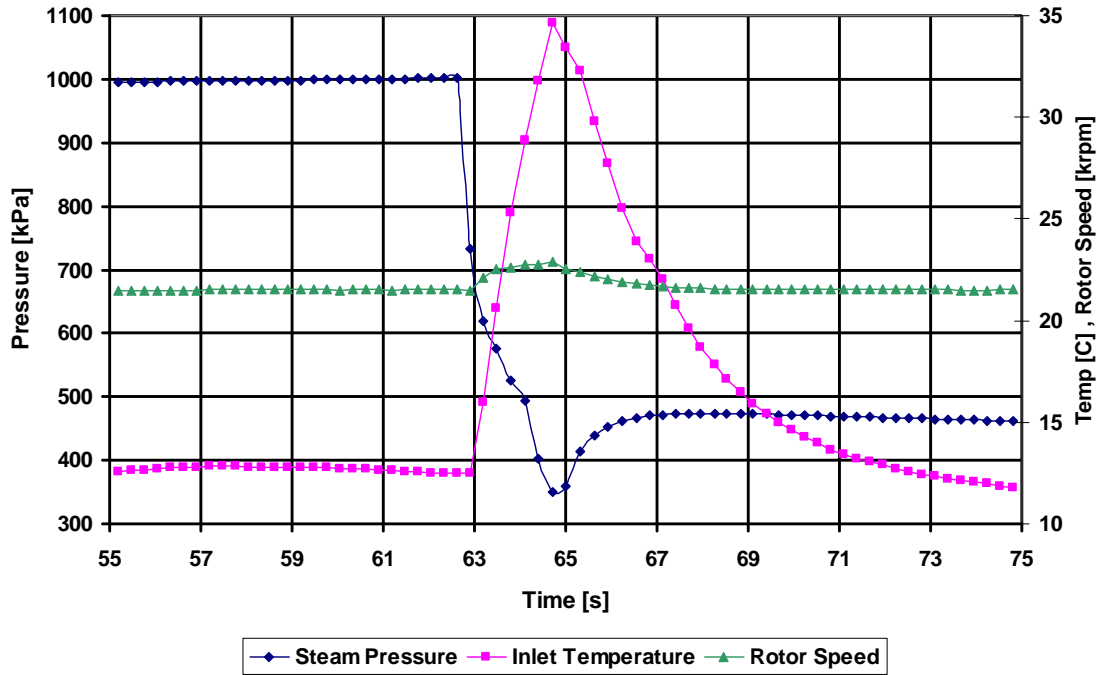


Figure 11. Steam Ingestion Time Trace

C. HIGH-SPEED INSTRUMENTATION RESULTS

1. Steady State Contour Plots

Data from the Kulite pressure transducers was interpolated over cross-sections of the rotor to create pressure contour maps at points of interest along each constant speed line. The MATLAB code used to accomplish the interpolation process was provided by Anthony Gannon [6] and is included in Appendix B. The best results were achieved when the interpolation was performed parallel to the shockwave preceding the leading edge of the rotor blade and perpendicular to the blade surface in the passage [2]. The contour plots featured in Figure 12 are examples of the pressure data taken prior to throttle-induced surge at each test speed.

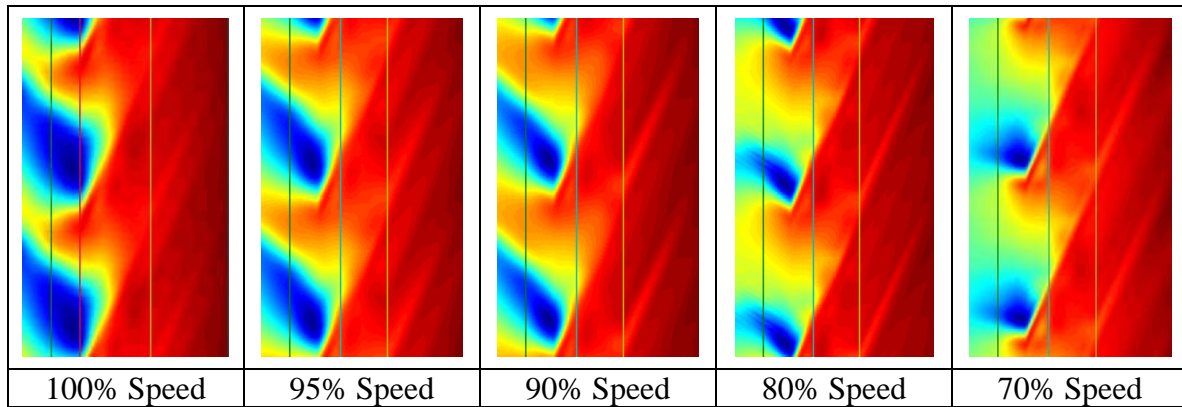


Figure 12. Interpolated Pressure Contour Maps Near Throttle-Induced Surge

When operating near open throttle conditions, it was shown that the stage configuration exhibited a tendency to produce normal shocks in the blade passage with oblique shocks forming at the leading edge of the rotor blade as expected in a transonic rotor. This observation even held true at 70% speed as localized regions of transonic flow allowed the formation of shocks despite a subsonic relative inlet velocity as shown in Figure 13. As the stage operating conditions approached the surge line, the formation of large detached bow shocks appeared when operating between 90% and 100% of the compressor design speed as shown for 95% speed in Figure 14. The pressure contour progressions for the remaining test speeds were included in Appendix C.

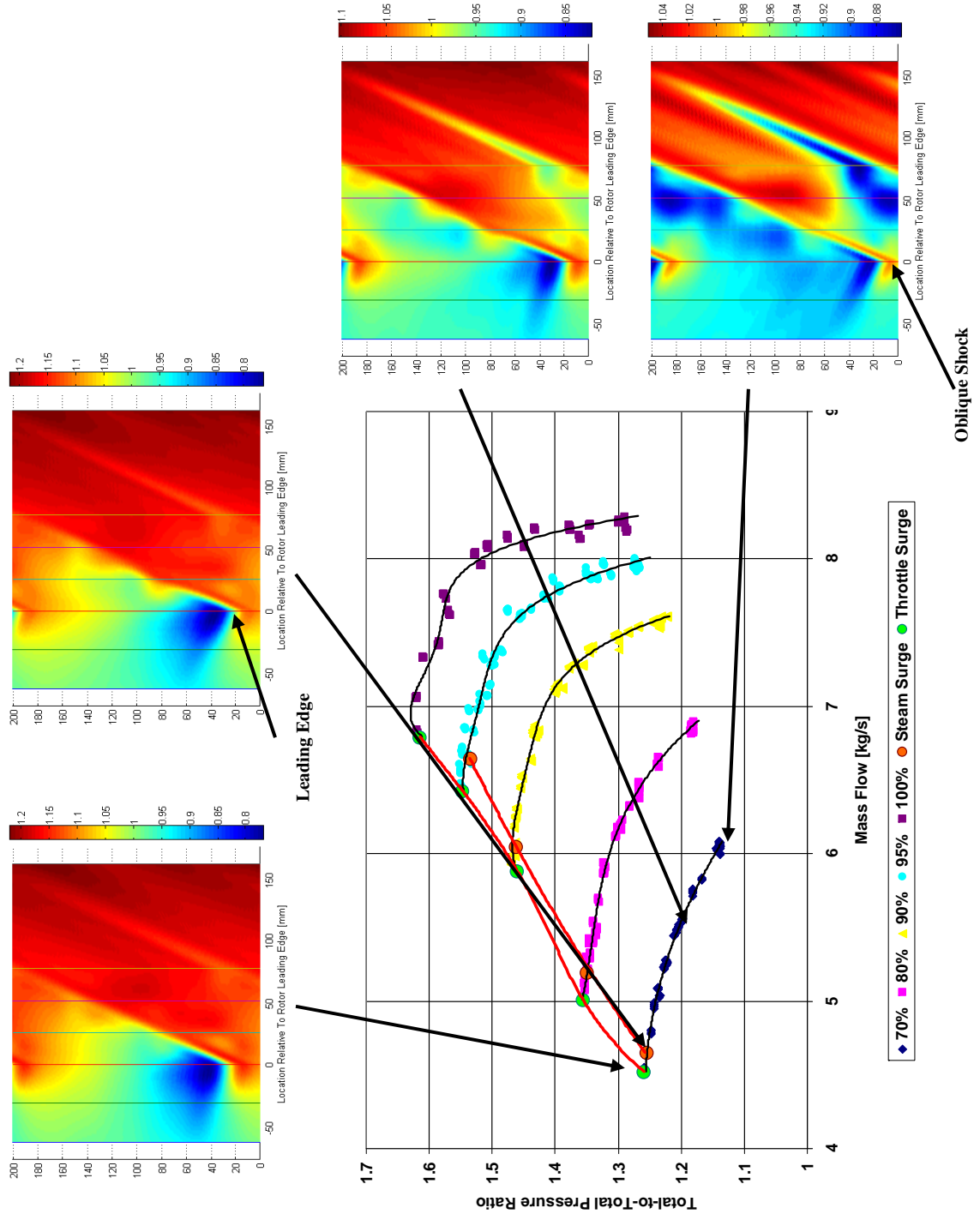


Figure 13. Pressure Contour Plot Progression for 70% Compressor Speed

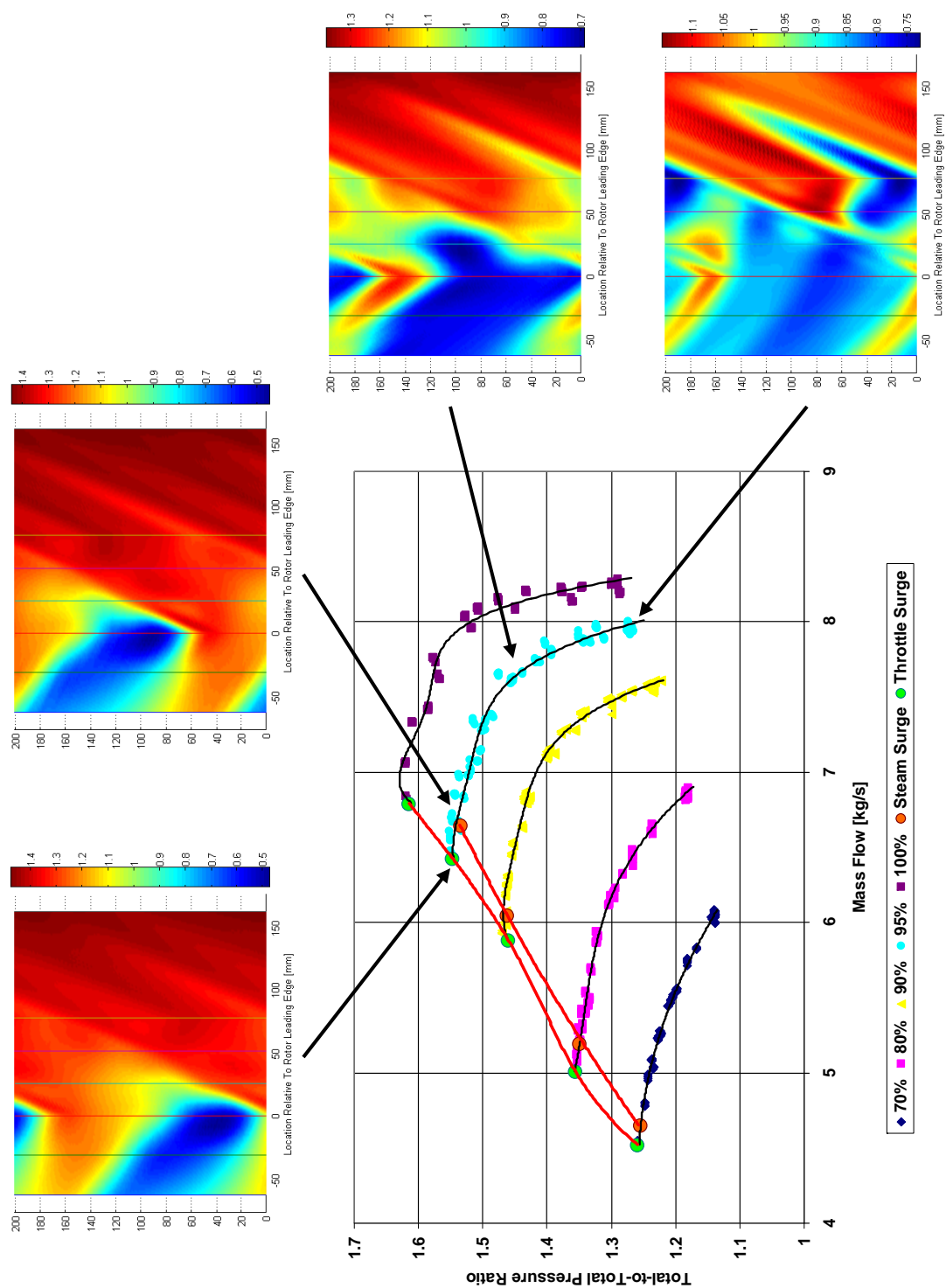


Figure 14. Pressure Contour Plot Progression for 95% Compressor Speed

2. Kulite Transient Data

Figures 15 and 16 contain examples of the raw voltage signal received from the Kulites during a surge event and the corresponding changes in rotor speed. The voltage oscillations observed in Figure 15 were indicative of the periodic nature of surge and offered a convenient means of determining the number of stall cycles that occurred during a surge event. Figure 16 provides an example of the plots utilized to determine the extent of the rotor overspeed during surge events, and the resulting overspeed values were then documented in Table 4. The raw voltage plots and rotor speed plots for throttle-induced surge and steam-induced surge events are contained in Appendix D. The MATLAB code used to produce these plots was provided by Anthony Gannon and is also included in Appendix D.

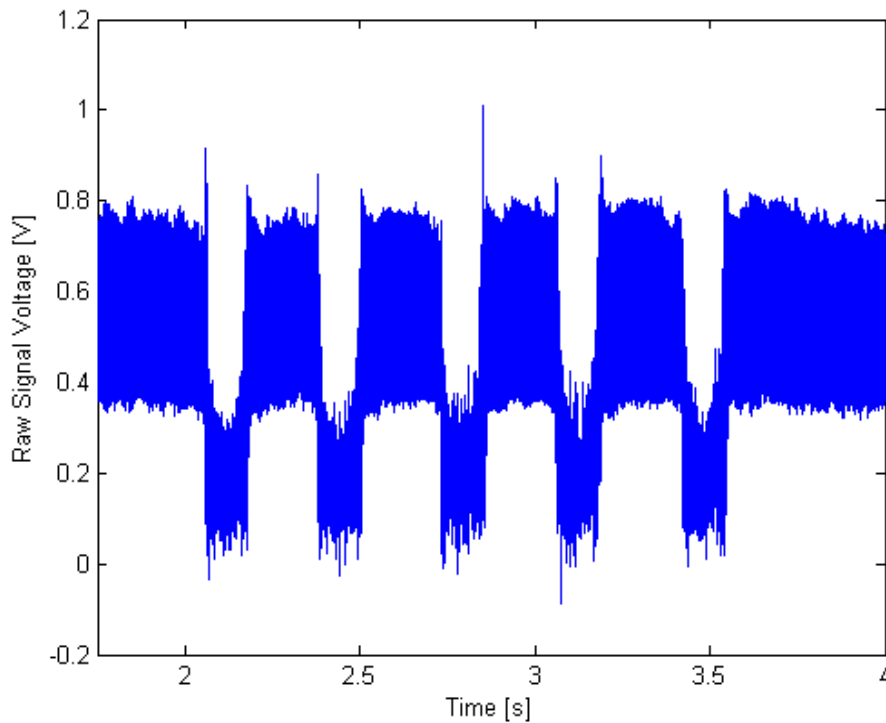


Figure 15. Example Plot of Raw Kulite Voltage During Steam Surge

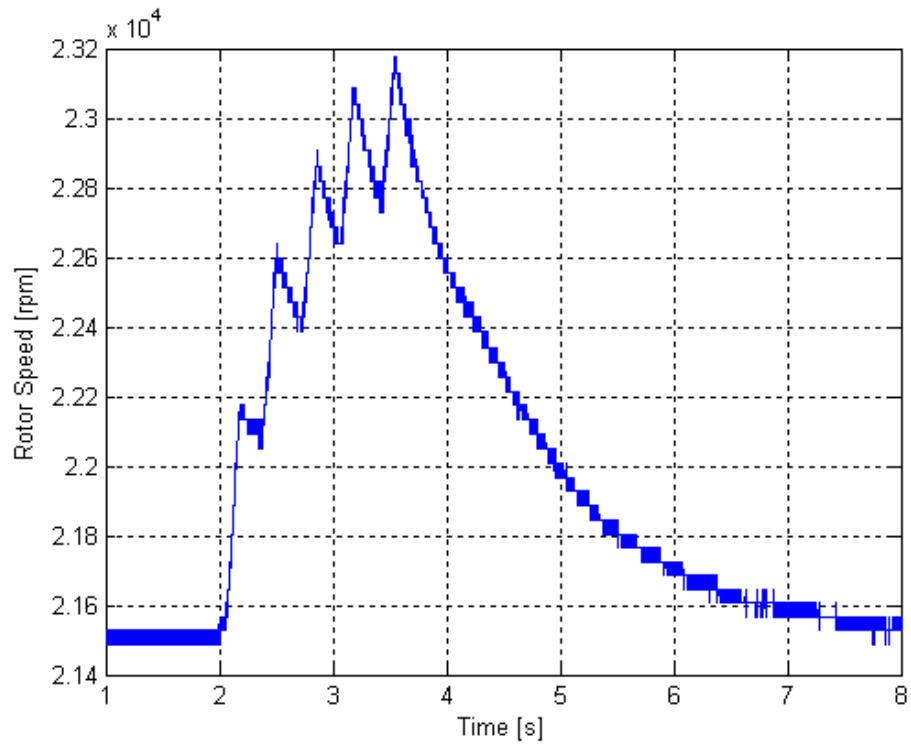


Figure 16. Example Plot of Rotor Speed During Steam Surge

Table 4. Rotor Overspeed Comparison

Rotor Speed	Expected Rotor RPM	Throttle Overspeed	Steam Overspeed
70%	18,960	3.3%	6.3%
80%	21,670	4.6%	7.6%
90%	24,375	5.5%	8.6%
95%	25,730	6.2%	5.5%

THIS PAGE INTENTIONALLY LEFT BLANK

VI. CONCLUSIONS

The effect of steam ingestion on the surge margin for a transonic compressor stage was quantified for both steady-state and transient performance. The experimental results confirmed that high-pressure steam ingestion produced a negative effect on the observed stall margin of the transonic compressor stage. Because the pressurized steam decreased the density of the incoming flow while simultaneously increasing its temperature, the rotor was forced to overspeed as a result of the constant power constraint imposed by the drive turbine. The increased rotor speed altered the angle of incidence of the incoming flow on the blades which was likely the most influential factor in precipitating surge events. It was also observed from the experimental data that the inclusion of a stator in the current test apparatus caused stall to occur at a lower mass flow rate than previously documented in the rotor-only configuration. This result indicated that the stator blades were likely the element most susceptible to stall in the stage configuration.

The results of this experiment showed that the rotor overspeed was more pronounced during steam-induced surge than during throttle-induced surge. This outcome was expected as the rotor speed must adjust to accommodate the combined effect of occlusions caused by regions of stalled flow and a reduction in the density of the incoming flow as a result of steam ingestion. Another potential concern associated with steam-induced surge was the rapid increase in shaft torque and stress associated with the rotor overspeed. Due to the cyclic nature of surge, the shaft experiences sharp speed gradients that contribute to increases in the shaft torque and large alternating stresses. Because stress varies with respect to the square of the rotor speed, even minor increases in the rotor speed during stalled operation can result in stress increases that pose a significant threat to sensitive components such as couplings and bearings.

THIS PAGE INTENTIONALLY LEFT BLANK

VII. RECOMMENDATIONS

The research conducted in this experimental investigation would likely benefit from the incorporation of a computational fluid dynamics (CFD) model to simulate the flow field in the transonic stage. A high-fidelity flow model would provide an efficient means to predict trends in the stage performance characteristics over a wide spectrum of operating conditions.

Additional improvements that would enhance future research include an increase in the sampling rate of the Kulite pressure transducers and an increase in the number of Kulites employed in the axial direction. The current sampling rate of 19.8 readings per blade passage was relatively low for this application, and any increase in the sampling rate would likely translate into increased data accuracy during both steady state and transient operation. Increasing the Kulite density along the blade cross section would likely have an even greater impact as it would improve the resolution of the pressure data to be interpolated and result in higher quality pressure contour maps.

Analysis of modal instabilities present in the stage configuration was a possibility that was not considered in this study; however, the identification of stall precursors present in the transonic stage has the potential to yield information with practical applications in aircraft control systems. Information regarding the detection of stall precursors could potentially enable the design of control systems that actively monitor throttle settings during an aircraft launch to preempt conditions conducive to stall.

The generation of transient pressure contour maps monitoring the development of stall cells also warrants further investigation as they may reveal the factors contributing to surge initiation in the stage configuration. As revealed in studies of the rotor-only configuration by Gannon et al. [2], the development of transient pressure contour maps may reveal differences in the development of surge linked to variations in the compressor speed.

THIS PAGE INTENTIONALLY LEFT BLANK

LIST OF REFERENCES

- [1] N.A. Cumpsty, Compressor Aerodynamics, New York : Longman Scientific & Technical, 1989.
- [2] A.J. Gannon, G.V. Hobson, R.P. Shreeve, and I.J. Villescas, “Experimental Investigation During Stall and Surge in a Transonic Rotor Fan Stage & Rotor Only Configuration,” ASME GT2006-90925 , Proceedings of TURBO EXPO. Barcelona, Spain, May 2006.
- [3] A.J. Gannon, G.V. Hobson, T.A. Payne, and S.E. Zarro, “The Effect of Steam Ingestion on Transonic Rotor Stall Margin,” ASME GT2007-28068. Proceedings of TURBO EXPO. Montreal , Canada, May 2007.
- [4] A.J. Gannon and G.V. Hobson, “Pre-Stall Modal Instabilities In A Transonic Compressor Rotor.” ISABE-2007-1348. Proceedings of ISABE 2007. Beijing, China, September 2007.
- [5] A.J. Gannon and G.V. Hobson, “Pre-Stall Instability Distribution Over a Transonic Compressor Rotor.” ASME GT2008-51512. Proceedings of TURBO EXPO. Berlin, Germany, June 2008.
- [6] Gannon, A.J., “Main.m” Private Communication, MATLAB code. March, 2008.
- [7] P. Hill and C. Peterson, Mechanics And Thermodynamics of Propulsion. Massachusetts: Addison-Wesley Publishing Company, Inc., 1992.
- [8] J.J. Koessler, Experimental Investigation of High-Pressure Steam Induced Stall of a Transonic Rotor. Master’s Thesis. Naval Postgraduate School, Monterey, California, June 2007.
- [9] B. Lakshminarayana,. Fluid Dynamics and Heat Transfer of Turbomachinery. New York : John Wiley & Sons, Inc., 1996.
- [10] T.A. Payne, Inlet Flow-Field Measurements of a Transonic Compressor Rotor Prior to and During Steam-Induced Rotating Stall. Master’s Thesis. Naval Postgraduate School, Monterey, California, September 2005.
- [11] N.I. Sanger, “Design of a Low Aspect Ratio Transonic Compressor Stage Using CFD Techniques.” ASME Journal of Turbomachinery. Vol. 118. July, 1996, pp. 479-491.
- [12] N.I. Sanger, Design Methodology For The NPS Transonic Compressor. Naval Postgraduate School. Monterey, California, 1999.

- [13] S.E. Zarro, Steady-State and Transient Measurements Within a Compressor Rotor During Steam-Induced Stall at Transonic Operational Speeds. Master's Thesis. Naval Postgraduate School, Monterey, California, September 2006.

APPENDIX A: STEAM INGESTION TIME TRACES

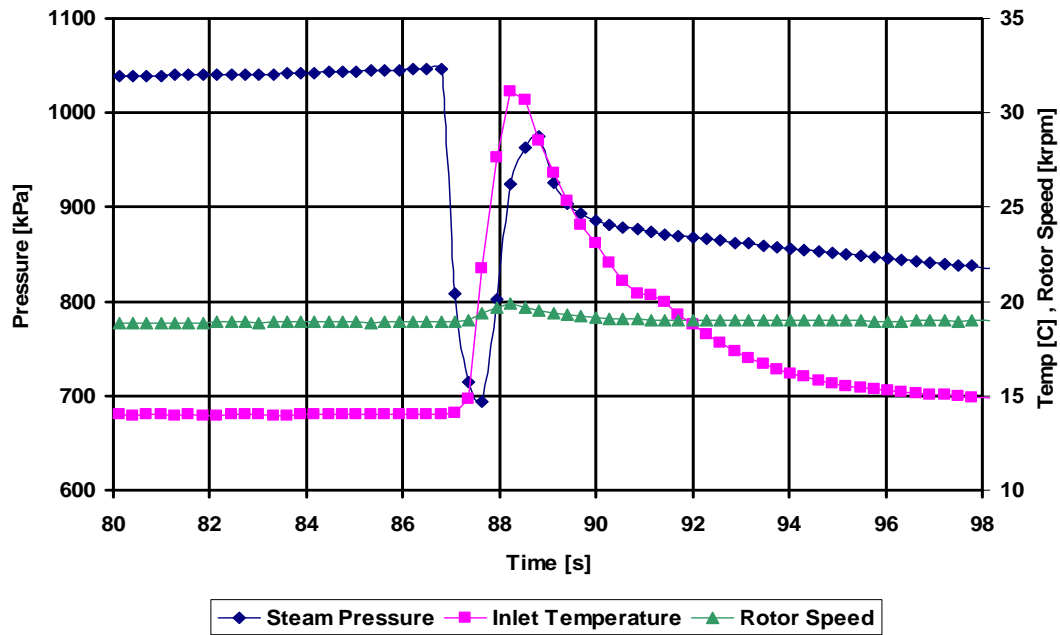


Figure 17. 70% Steam Induced Surge

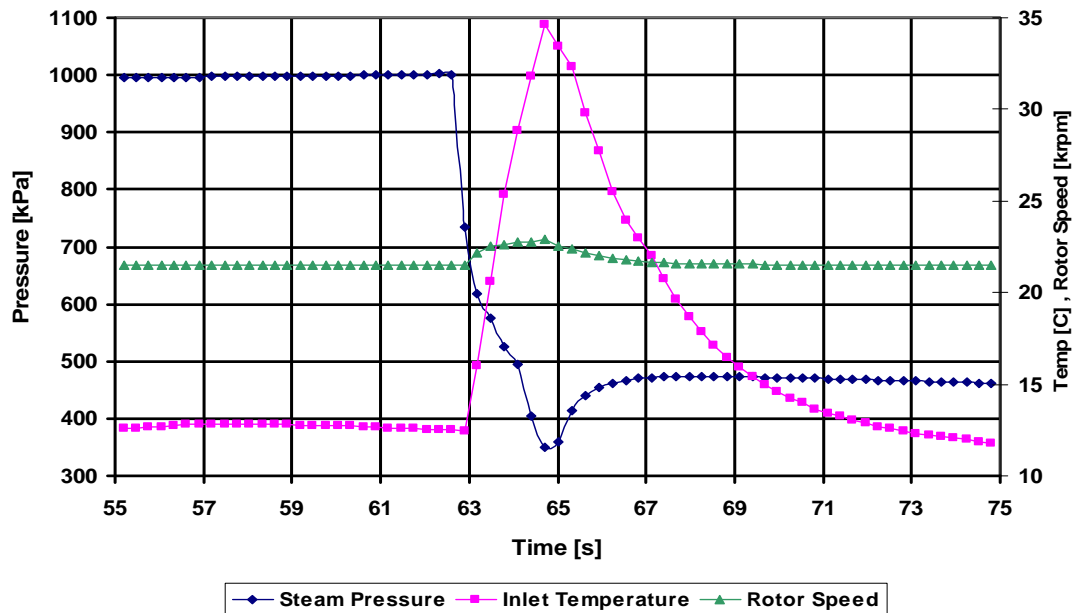


Figure 18. 80% Steam Induced Surge

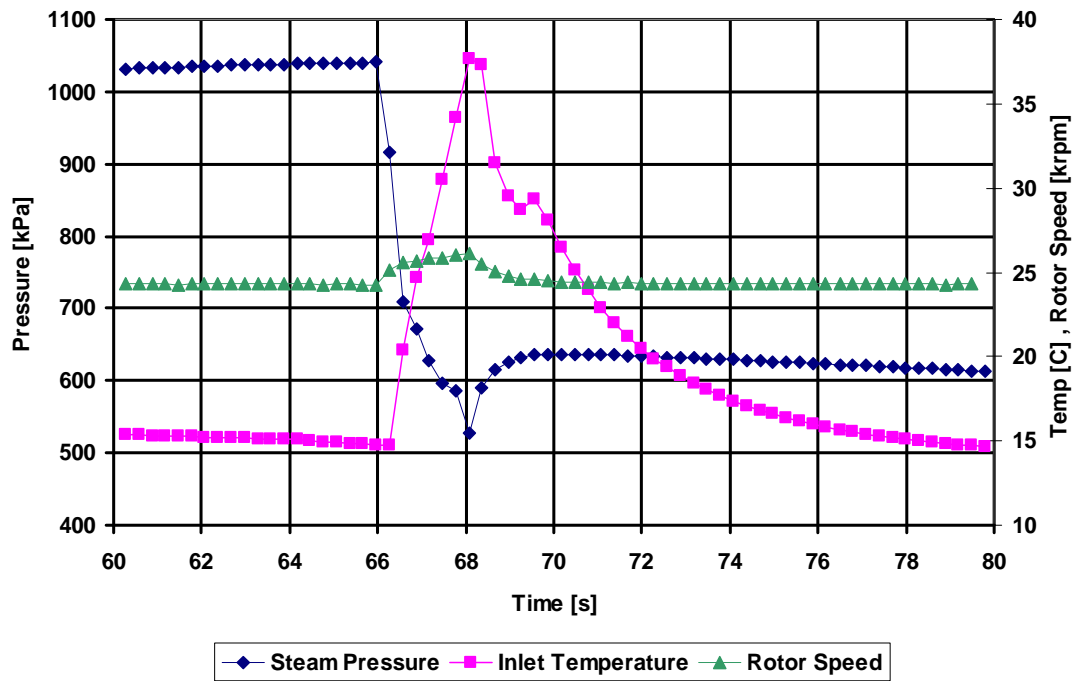


Figure 19. 90% Steam Induced Surge

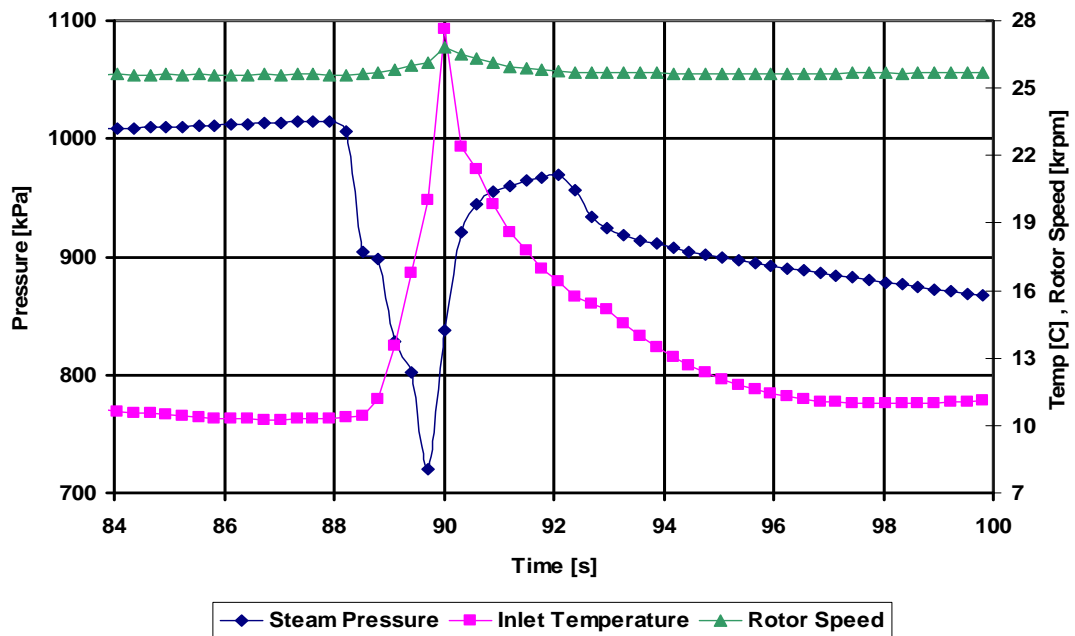


Figure 20. 95% Steam Induced Surge

APPENDIX B: MATLAB CODES USED TO PROCESS KULITE DATA

Instructions:

1. Change MATLAB working directory to the desired stage data folder
2. Copy Main.m into the current working directory
3. Change the Kulite data file name to reflect the date, speed, and run to be processed
4. Enter Main.m in the workspace command window
5. The process should take several minutes to complete

Main.m:

% m-file to plot the Kulite contours for the rotor only case with 7 Kulites

clear all

% Kulite data filename

Kulite_constants = 'Kulite_constants_100_2008_02_08_stage_Run_21'; % 100% near peak efficiency

%Kulite_constants

% Kulite constant file is initialized

%eval(Kulite_constants)

% Raw data is loaded in a separate function file and also calibrated to make the analysis function neater

[time,tach,samples,P_PR,P_PR_stall,m_dot_REF,PR_REF,RPM_sample]

Load_Kulite_Data(Kulite_constants);

% Function to find the position of the trigger signal, the trigger level and the Hz frequency of revolution

[Loc,HZ,Trig] = Process_Kulite_Data(tach,samples,time);

% Function to correct the times to phase the Kulites over the blades and correct for errors in the triggers

[time_phase,time_err,time_angle,P_PR]

Phase_Kulite_Data(Kulite_constants,Loc,HZ,tach,time,P_PR);

% Function to put all the data into single time traces over ONE ROTATION and also ONE PASSAGE as if it was sampled at very high speed

[time_rev,P_PR_rev,time_passage,P_PR_passage]

Rot_Kulite_Data(Kulite_constants,HZ,Loc,time,time_err,time_phase,P_PR);

```

% Function to find the moving averages of the data to smooth it out (quadratic function is
used to ensure that peak clipping does not occur)
[P_PR_bin,P_PR_bin_DELTA,time_bin]
Avg_Kulite_Data(Kulite_constants,time_rev,P_PR_rev,HZ,0);

% Function to find the moving averages of the data to smooth it out but for one averaged
blade passage
[P_PR_bin_passage,P_PR_bin_passage_DELTA,time_bin_passage]
Avg_Kulite_Data(Kulite_constants,time_passage,P_PR_passage,HZ,0);

% Function to interpolate in the axial direction over a single blade passage
[contour_z_passage,contour_th_passage,contour_PR_passage]
Contour_Kulite_Data(time_bin_passage,P_PR_bin_passage,HZ,time_angle,Kulite_constants);

% Function to interpolate in the axial direction over the entire rotor
%[contour_z_rotor,contour_th_rotor,contour_PR_rotor]
=Contour_Kulite_Data(time_bin,P_PR_bin,HZ,time_angle,Kulite_constants);

% Data is saved and then loaded so that the whole thing does not have to be run again
save Kulite

%Save_Kulite_Data(Kulite_Subdir,Kulite_Run_no,'save') % Data is saved in raw data
directory
Save_Kulite_Data('save',Kulite_constants) % Data is saved in raw data directory

Kulite_figures_rotor_only(Kulite_constants)

```

APPENDIX C: PRESSURE CONTOUR PLOTS

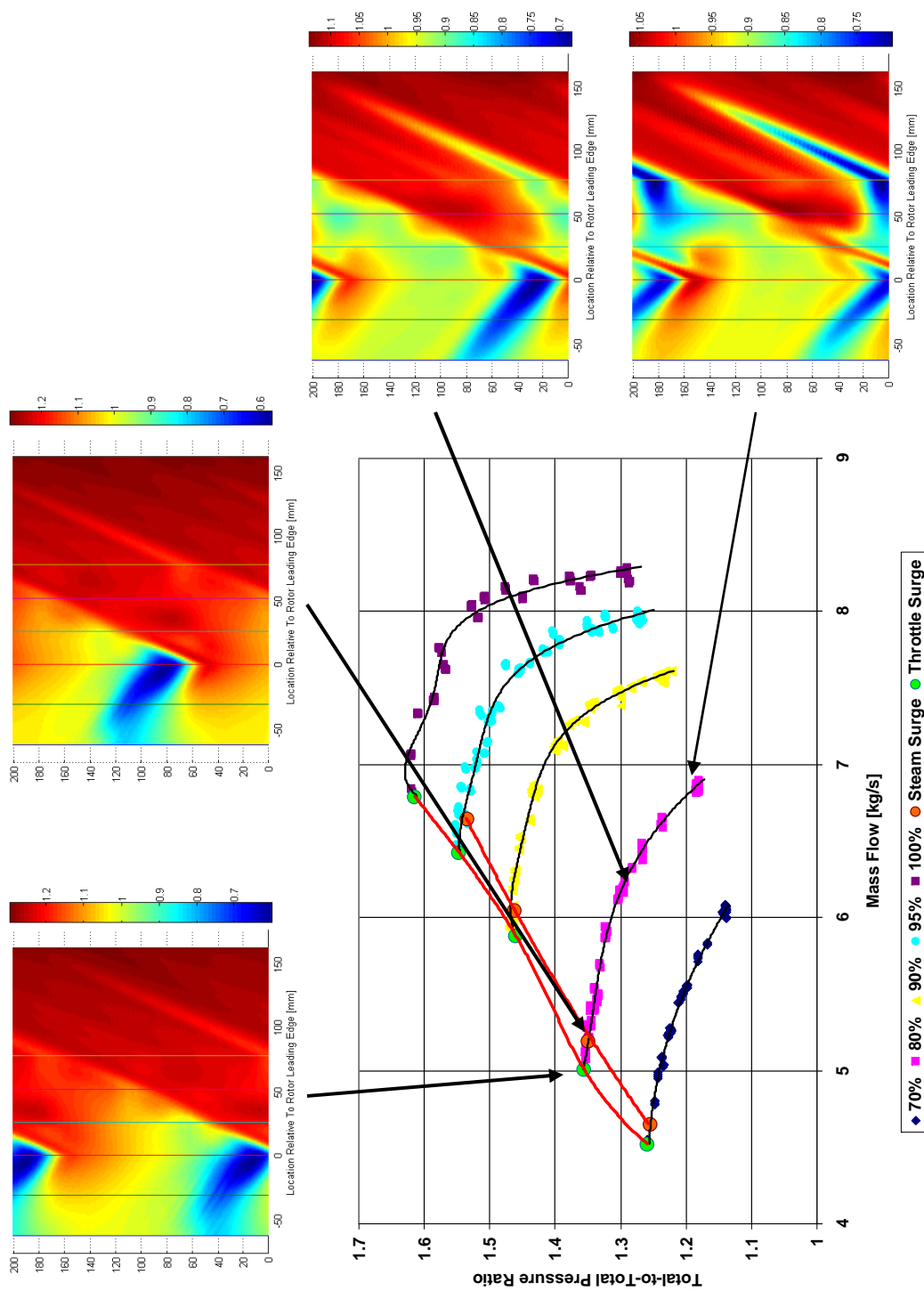


Figure 21. Pressure Contour Plot Progression for 80% Compressor Speed

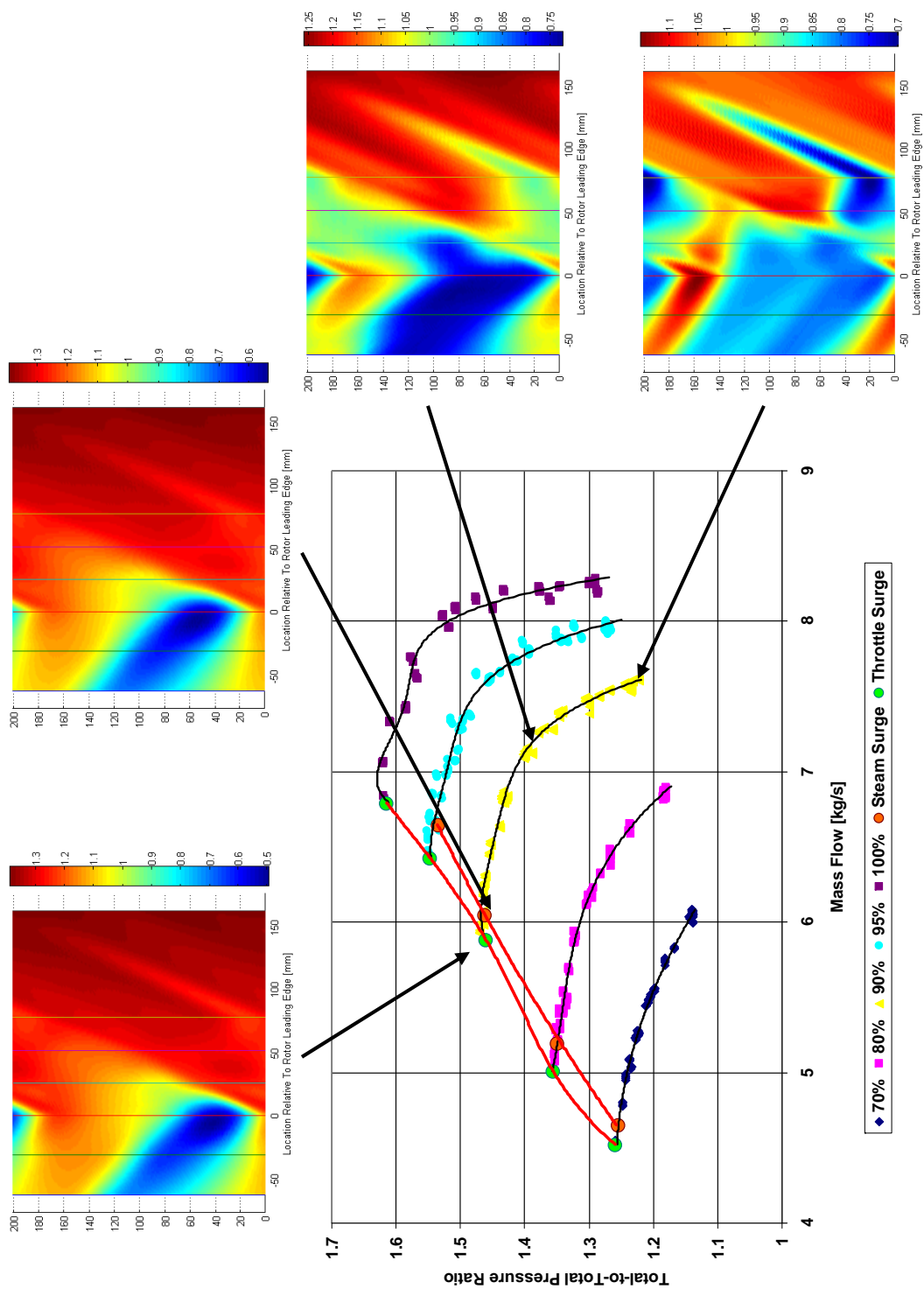


Figure 22. Pressure Contour Plot Progression for 90% Compressor Speed

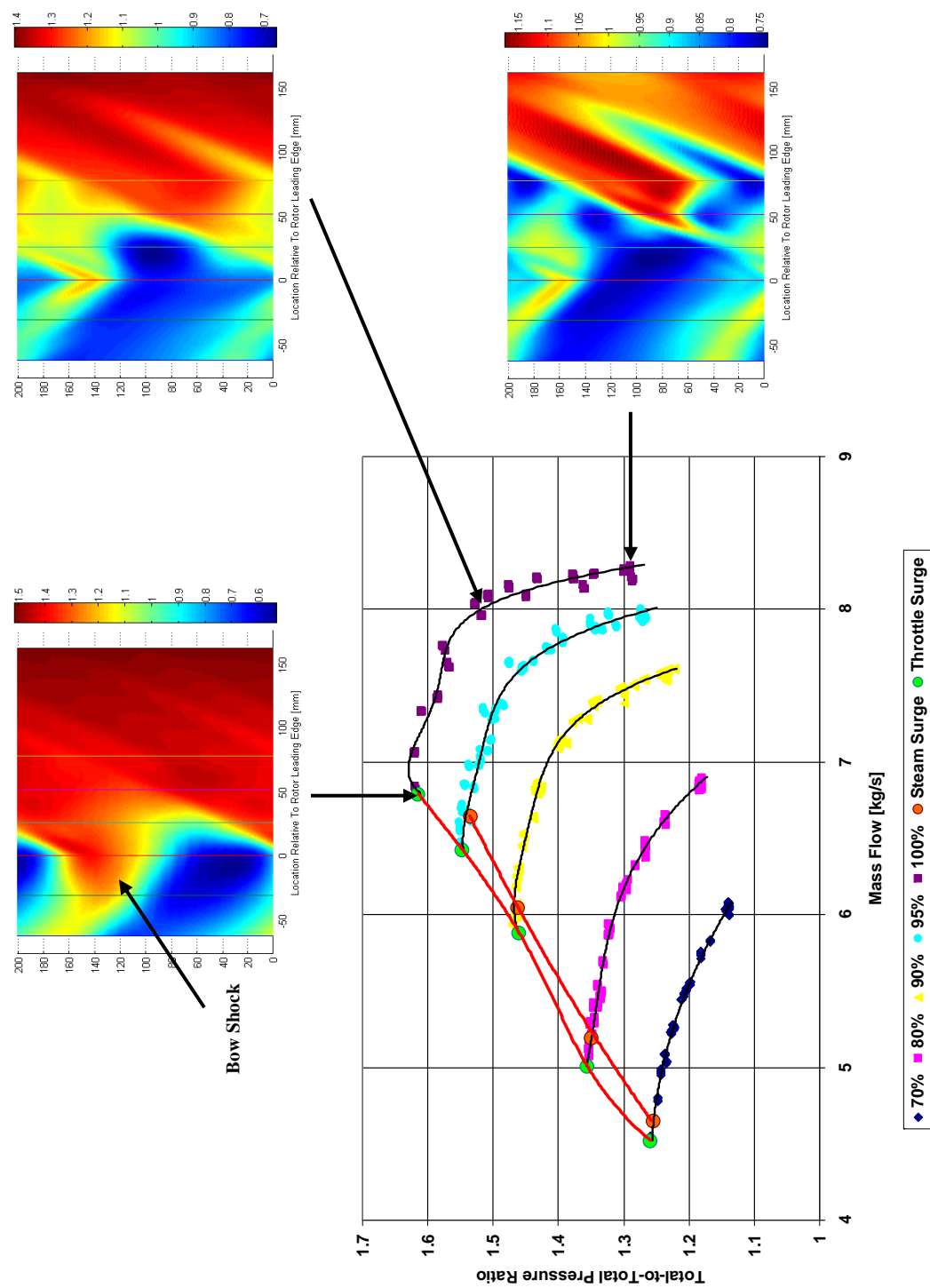


Figure 23. Pressure Contour Plot Progression for 100% Compressor Speed

THIS PAGE INTENTIONALLY LEFT BLANK

APPENDIX D: KULITE SIGNAL VOLTAGE AND ROTOR OVERSPEED DURING SURGE

Instructions:

1. Open directory containing the Kulite stall data
2. Copy Main.m into the current directory
3. Change the Raw_data entry to the desired Kulite stall data file in Main.m
4. Enter Main.m in the workspace command window
5. The process should take several minutes to complete

Main.m:

% M-file to do basic data review from Kulites

clear all
close all

% Load time data
Raw_data = dlmread('Dx2008_0228_95_stall.csv',',',5,0);

% Strip out time
time = Raw_data(:,1);

% Strip out once per rev
Tach = Raw_data(:,14);

% Strip out hotwire voltages
Hot_wire = Raw_data(:,12:13);

% Strip out Kulite voltage
Kulite = Raw_data(:,2:11);

% Trigger level is simply mean of max and min
Trig = mean([min(Tach) max(Tach)]);

% Location of trigger
Loc = find(Tach(2:end)<Trig & Tach(1:end-1)>Trig); %location of time of start of rev

% Frequency of rotor revolution over the sample periods
Hz = 1./(time(Loc(2:end))-time(Loc(1:end-1)));
RPM = Hz*60;

% Smoothed RPM
RPM_smooth = RPM;
for i = 1:3

```

    RPM_smooth = [RPM_smooth(1); RPM_smooth(2:end)-diff(RPM_smooth)/2];
end

% plot once per rev
figure(1); close; figure(1);
title('Raw Tach Signal')
plot(time,Tach); hold on
plot(time(Loc),Tach(Loc),'+r')

% Plot of RPM
figure(2); close; figure(2);
title('RPM')
h1 = plot(time(Loc(2:end)),RPM,'b'); hold on
h2 = plot(time(Loc(2:end)),RPM_smooth,'r');
grid on

% Plot of hotwire voltage
figure(3); close; figure(3);
title('Hotwire Voltage')
h3 = plot(time,Hot_wire); hold on; hold on

% Plot of Kulite voltage
figure(4); close; figure(4);
title('Kulite Voltage')
h3 = plot(time,Kulite(:,1:3)); hold on; hold on

```

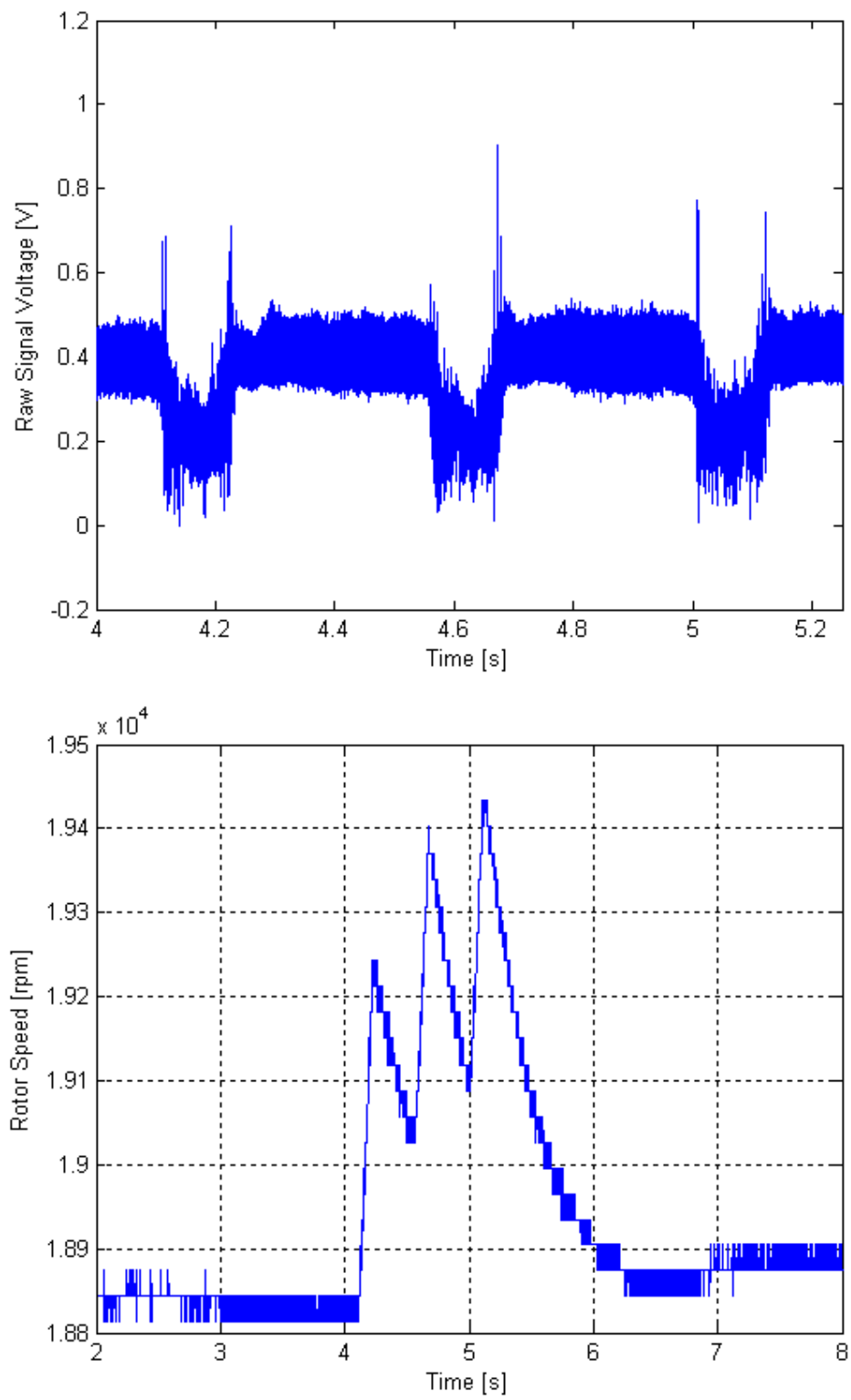



Figure 24. 70% Throttle-Induced Surge

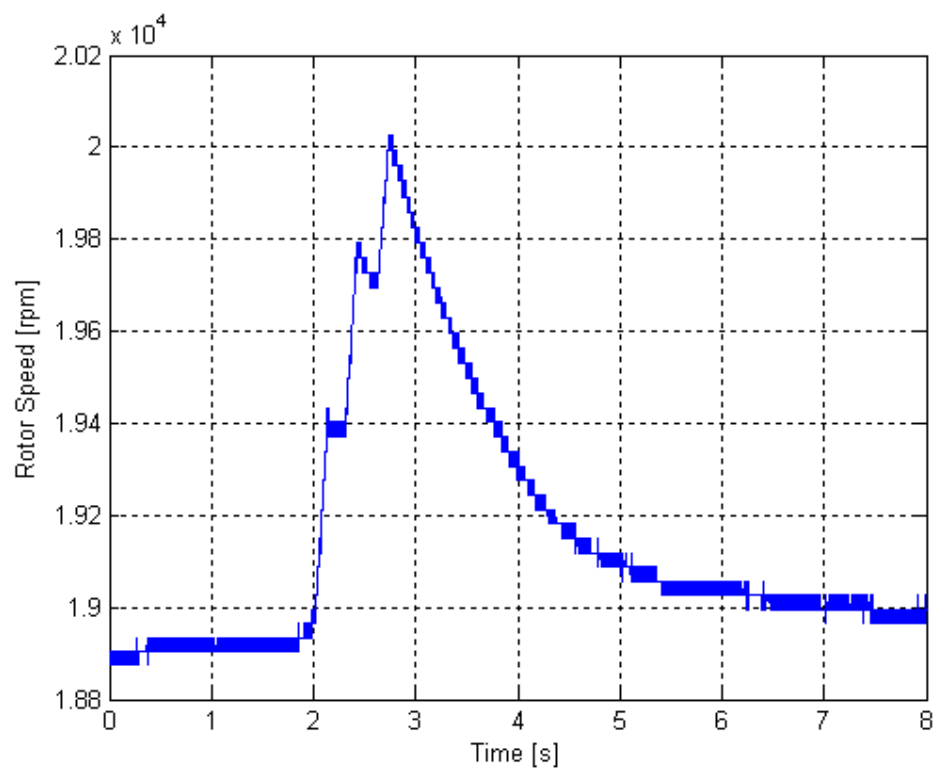
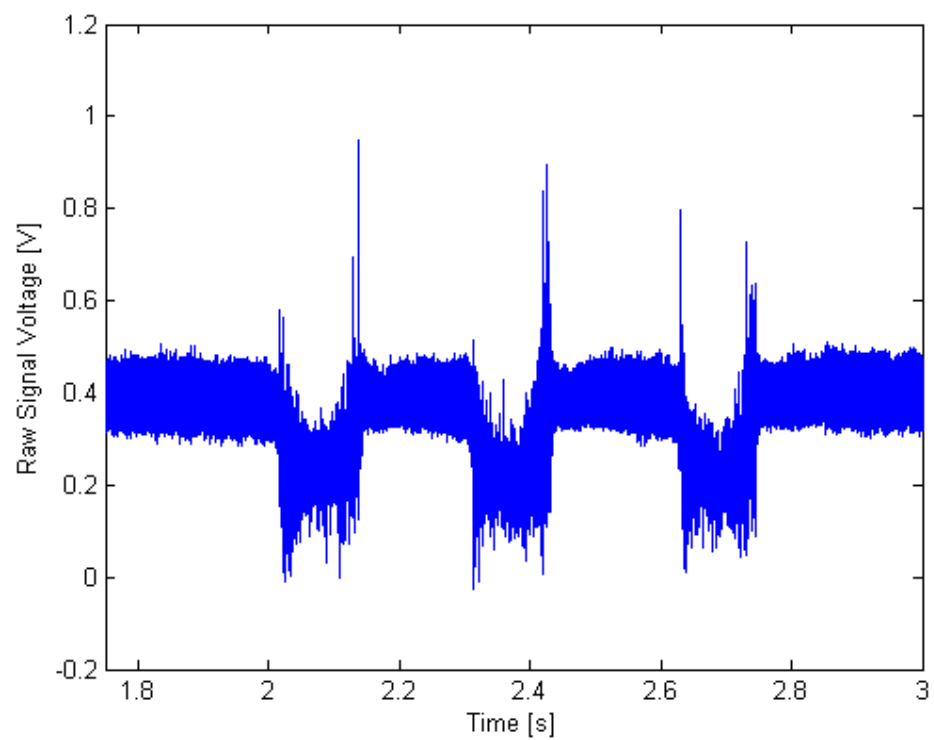


Figure 25. 70% Steam-Induced Surge

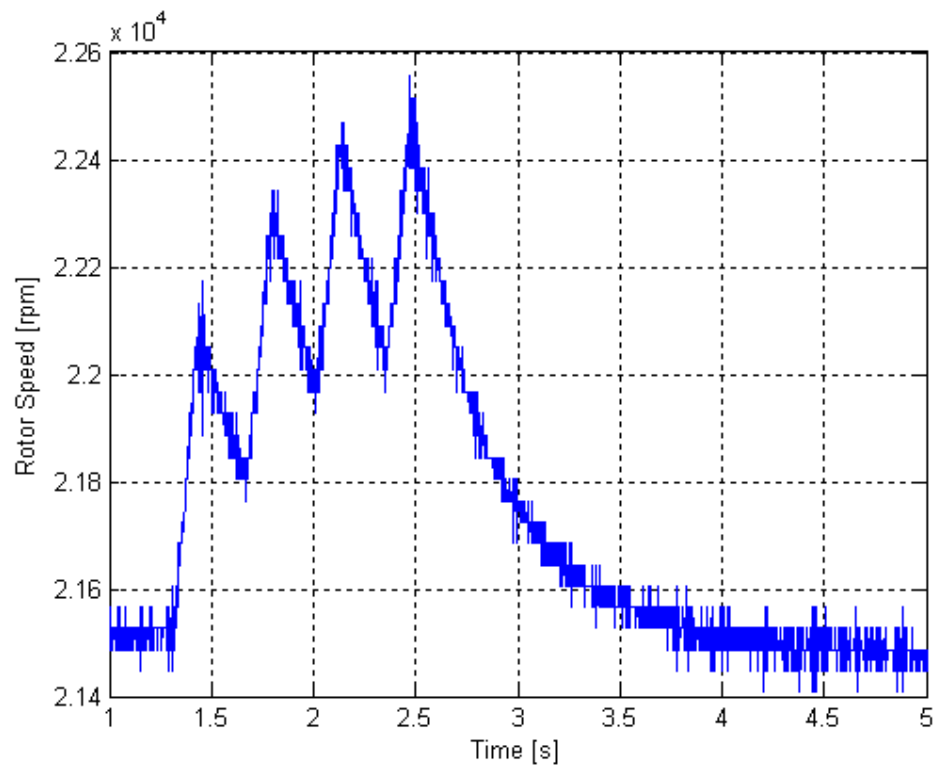
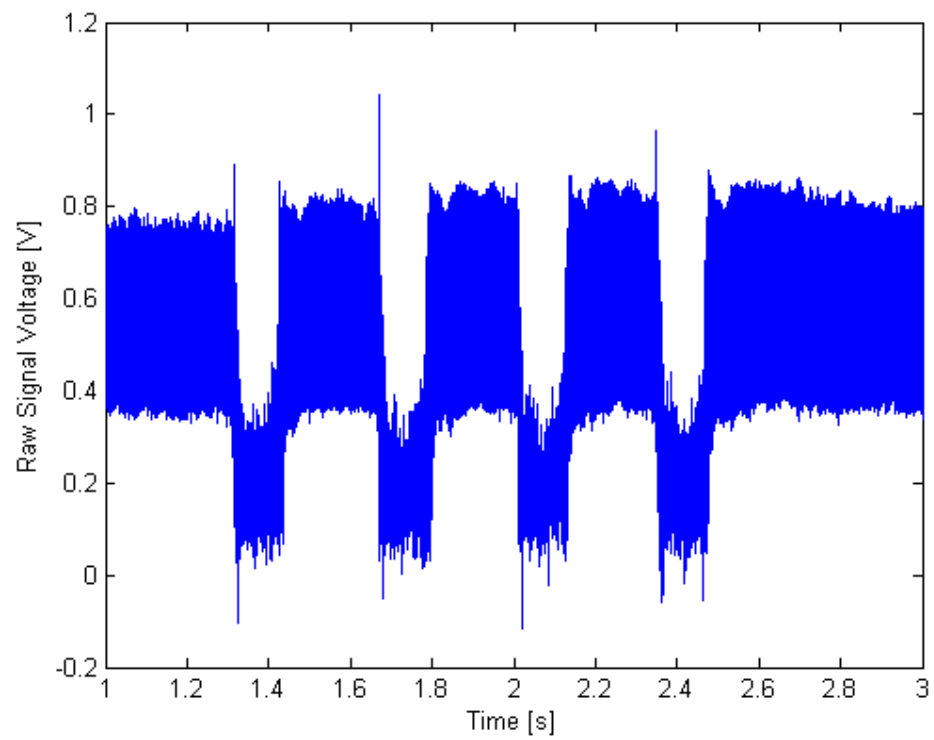


Figure 26. 80% Throttle-Induced Surge

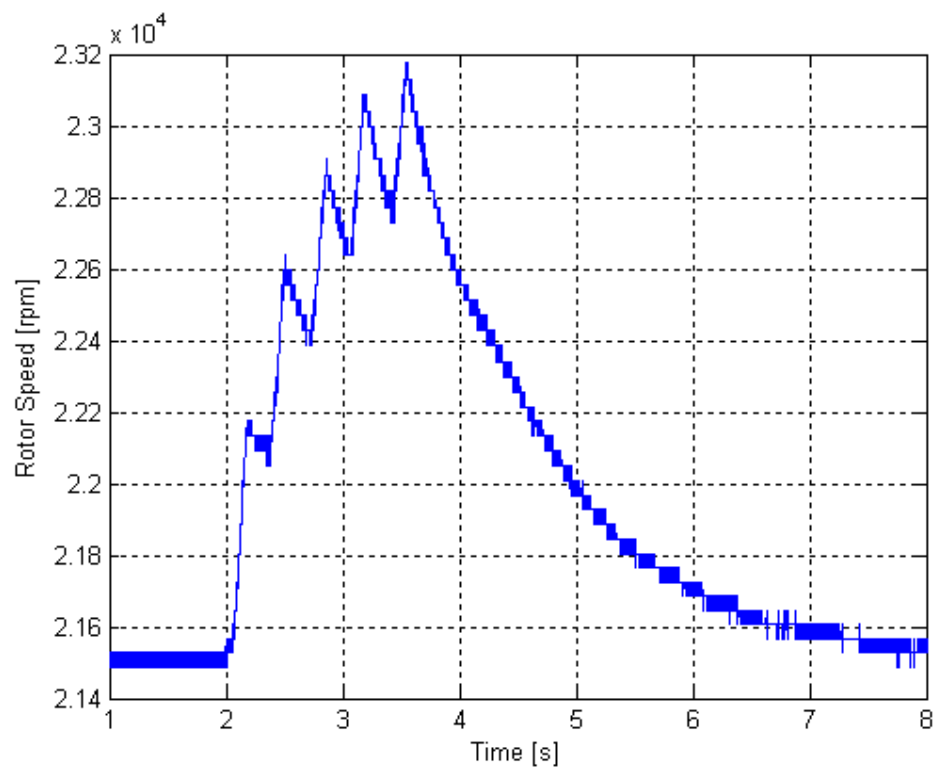
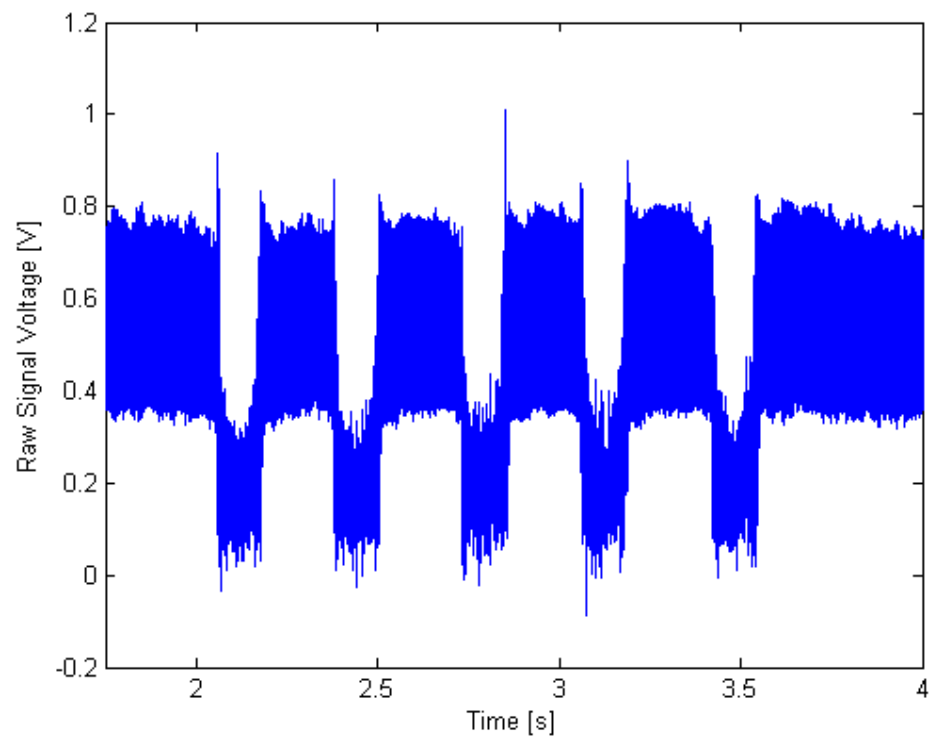


Figure 27. 80% Steam-Induced Surge
44

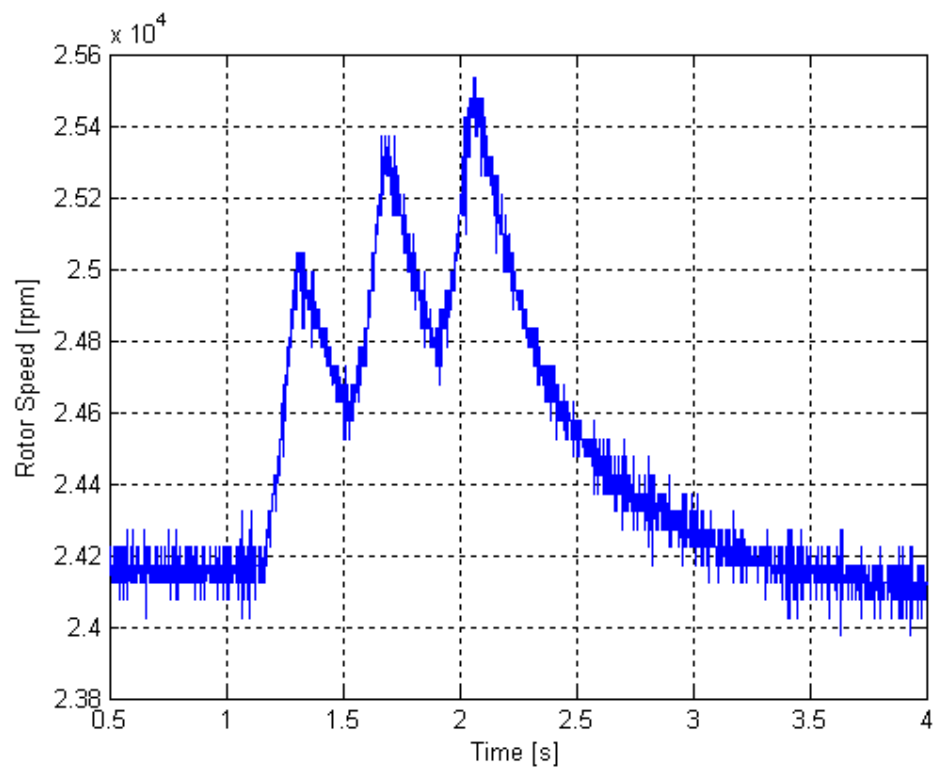
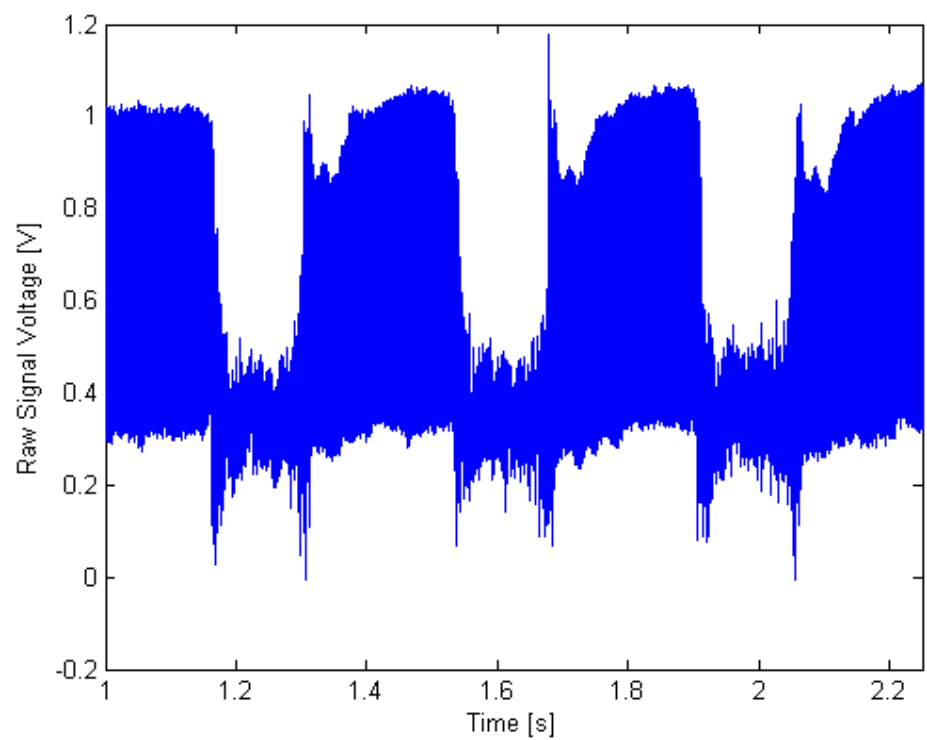


Figure 28. 90% Throttle-Induced Surge

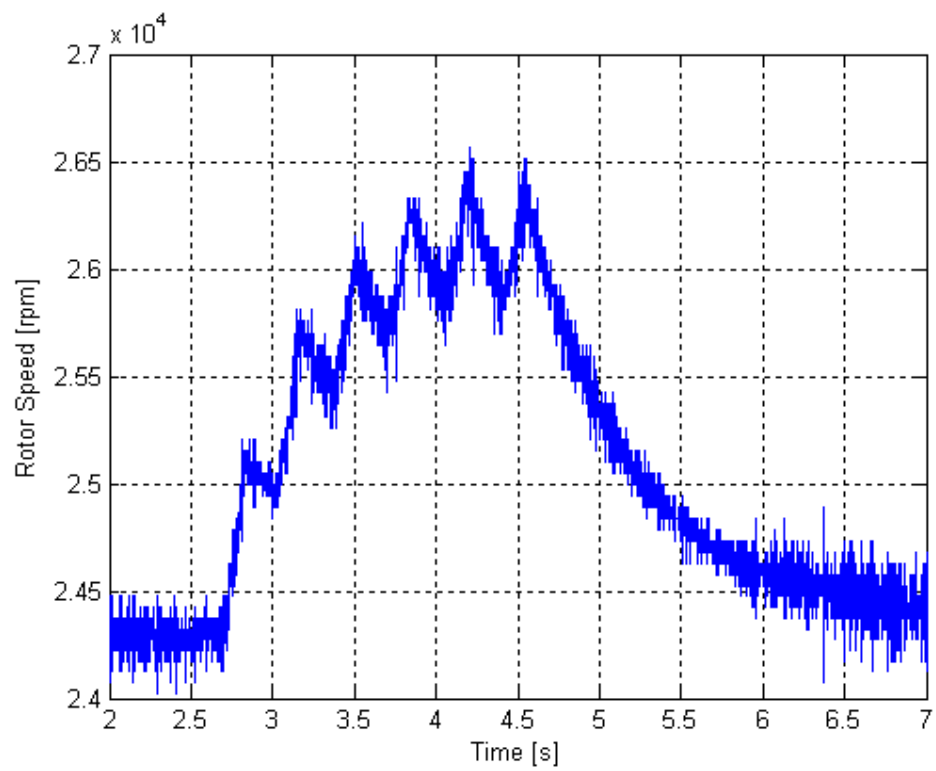
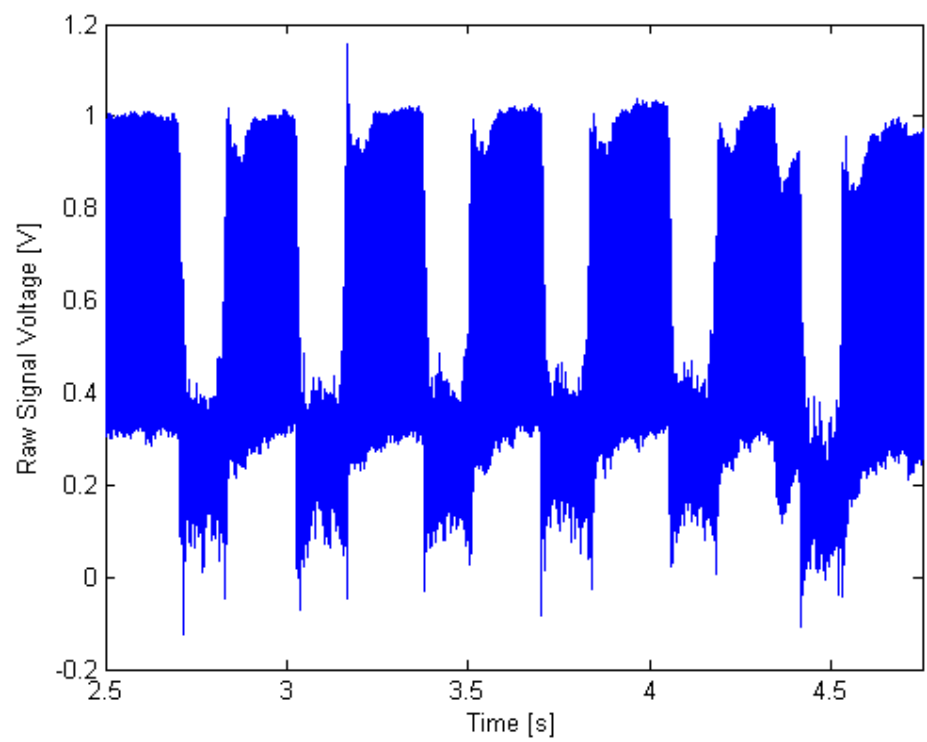


Figure 29. 90% Steam-Induced Surge
46

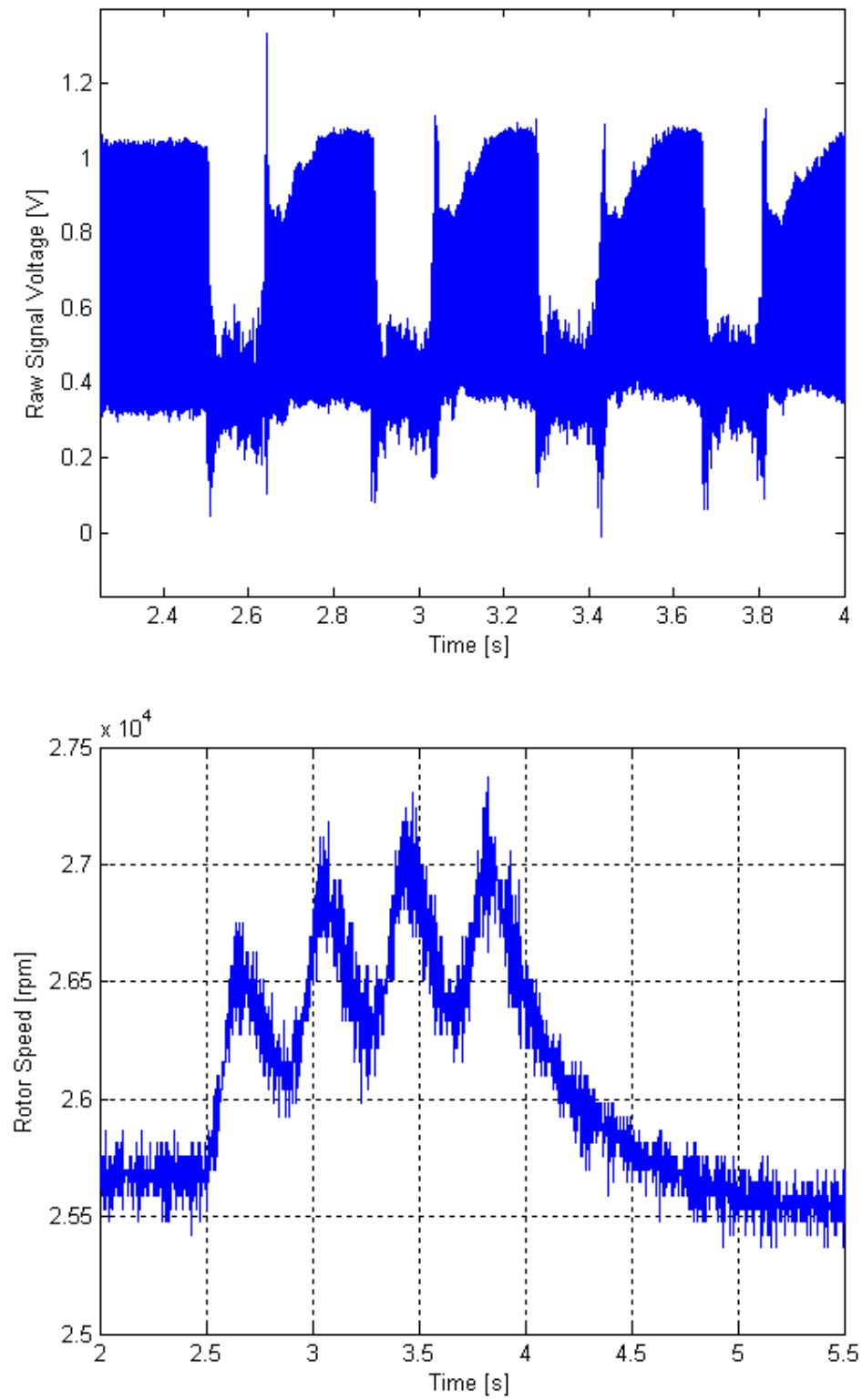


Figure 30. 95% Throttle-Induced Surge

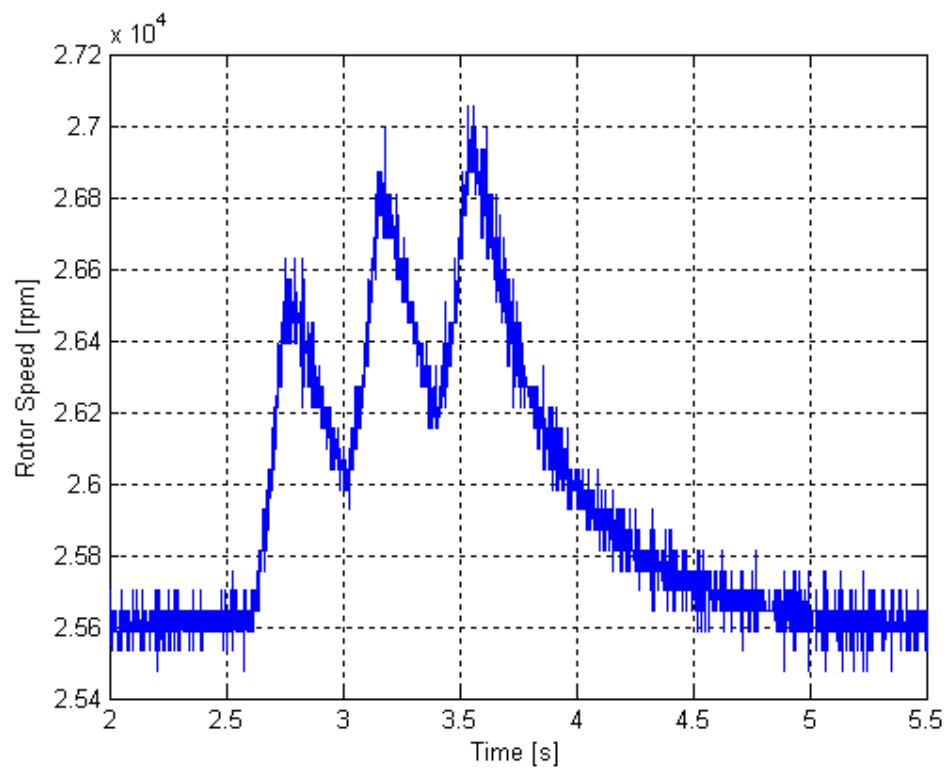
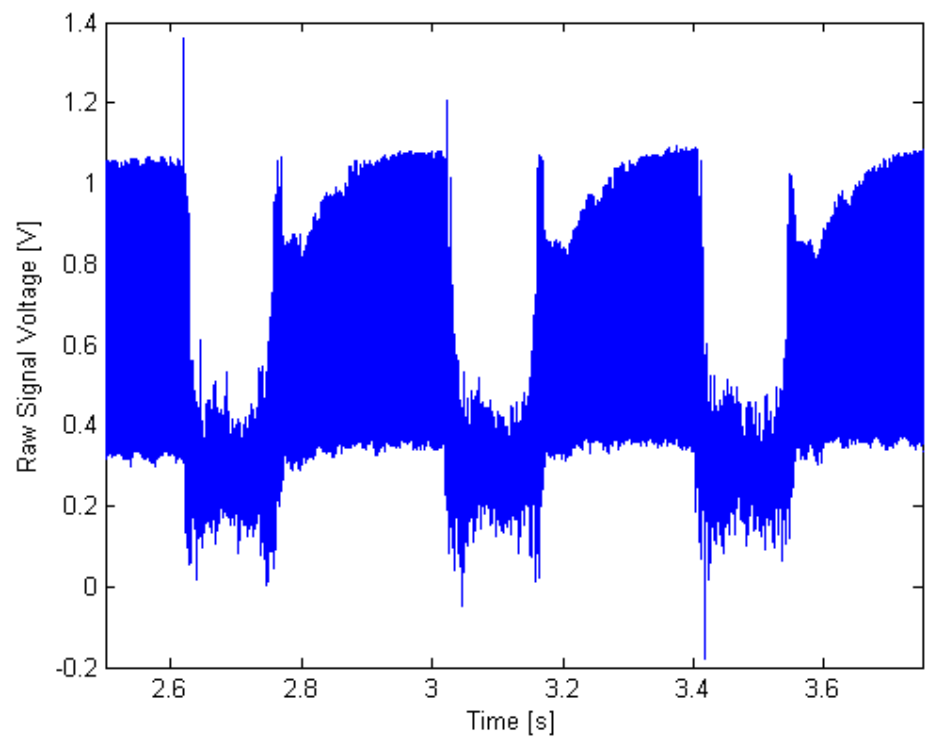


Figure 31. 95% Steam-Induced Surge
48

INITIAL DISTRIBUTION LIST

1. Defense Technical Information Center
Ft. Belvoir, Virginia
2. Dudley Knox Library
Naval Postgraduate School
Monterey, California
3. Distinguished Professor and Chairman Anthony Healey
Department of Mechanical and Aeronautical Engineering
Naval Postgraduate School
Monterey, California
4. Professor Anthony Gannon
Department of Mechanical Engineering and Aeronautical Engineering
Naval Postgraduate School
Monterey, California
5. Professor Garth Hobson
Department of Mechanical Engineering and Aeronautical Engineering
Naval Postgraduate School
Monterey, California
6. ENS Andrew Hurley
Monterey, California